Nonlinear Aeroelasticity

Earl Dowell
Duke University, Durham, North Carolina 27708
John Edwards
NASA Langley Research Center, Langley, Virginia 23681
and
Thomas Strganac
Texas A&M University, College Station, Texas 77843-3141

Introduction

THERE has been high interest and activity in the study of non-linear aeroelasticity for the last decade and more, and the literature is now extensive. In this paper, the authors' goal is to provide a faithful account of the state of the art as of this writing with an emphasis on key ideas and results that demonstrate our current theoretical, computational, and experimental capabilities and the degree to which correlation among results from these several approaches agree or disagree. An exhaustive literature survey is not attempted here; however, a bibliography of over 800 citations is available in electronic form from the first author on request. The particular results and methods described must inevitably reflect the authors' knowledge and experience, but we have made an effort to be comprehensive in terms of ideas and representative with respect to results insofar as possible.

The paper begins with a discussion of generic nonlinear aeroelastic behavior especially as it relates to limit cycle oscillations (LCOs); then the important studies that come from flight experience with

Earl H. Dowell's principal teaching interest and research activity is in the field of aeroelasticity, which is the study of the dynamic interaction between an aerodynamic flow and an elastic structure, such as aircraft wings in high-speed flight, long-span bridges, and tall buildings responding to wind loadings, or airflow through the mouth and lungs. Dowell has also done research in acoustics, nonlinear dynamics, structural dynamics, and unsteady aerodynamics. Major research accomplishments include the first definitive research monograph on the aeroelasticity of plates and shells, the first derivation and solution of the nonlinear equations of motion for a helicopter rotor blade (the Hodges–Dowell equations), and work with Kenneth Hall and several graduate students and postdoctoral fellows on reducing the dimensions of mathematical models for very complex high-dimensional fluid/structural systems. Dowell is a J. A. Jones Professor of Mechanical Engineering and Materials Science and teaches undergraduate and graduate courses on dynamics and aeroelasticity at Duke University. He is a member of the National Academy of Engineering and an AIAA Fellow.

John Edwards is a Senior Research Engineer in the Aeroelasticity Branch of NASA Langley Research Center. He has been with NASA since 1965: from 1965 to 1980 at the NASA Dryden Flight Research Center, and from 1980 to the present at the NASA Langley Research Center. He began his career in the area of flight control systems and has evolved through structural dynamics, unsteady aerodynamics, and aeroelasticity. From 1981 to 1989 he managed Langley's Unsteady Aerodynamics Branch. Dr. Edwards has a B.A. in physics from Yale University and a Ph.D. in aeronautics and astronautics from Stanford University. He is the author of over 70 technical publications in flight dynamics, structural dynamics, unsteady aerodynamics, and aeroelasticity. He has consulted in areas of aeroelastic limit cycle oscillations, tail buffeting and fatigue, the dynamics and resonances of transonic wind tunnels, and marine pump resonances. He is an AIAA Fellow.

Thomas Strganac is Associate Professor of Aerospace Engineering at Texas A&M University. Research interests focus on fluid-structure interaction, structural dynamics, nonlinear mechanics, material/system identification, and aeroelastic phenomena. His research, with the collaboration of his research assistants, has resulted in approximately 100 journal/other publications. He was a recipient of a National Science Foundation (NSF) CAREER award (formerly the NSF Young Investigator Award) with research focused in fluid-structure-control interaction and with CAREER education initiatives in new teaching hardware/pedagogy for the classroom. He has developed new courses including Structural Dynamics in Engineering Systems, Aeroelasticity, Aircraft Structural Analysis & Design, Unsteady Aerodynamics, and Nonlinear Dynamics and Chaos. He has organized and presented the short courses-Hazardous Flight Tests and Aeroelasticity. He is also a member of the instructor team for the AIAA Professional Development Course titled Aeroelasticity—State of the Art Practices. He is the co-author of the textbook Introduction to Flight Test Engineering (Kendall-Hunt, 3rd edition, 2002). In 2002 and 2003 he served a one year appointment as Visiting Scientist with the Air Force Research Laboratory at Wright–Patterson Air Force Base, Ohio. He served as the General Chairman of the AIAA's Structures, Structural Dynamics and Materials Conference in 1999. He served as the General Chairman of the AIAA's Dynamics Specialists Conference in 1996. He currently serves as an Associate Editor of the AIAA *Journal of Aircraft*. He is an Associate Fellow of AIAA and a registered professional engineer. Prior to his position at Texas A&M University, he served as a Research Engineer at NASA—Langley Research Center and as an Aerospace Engineer at NASA–Goddard Space Flight Center. He received his B.S. in aerospace engineering from North Carolina State University, his M.S. in aerospace engineering from Texas A&M University, and his Ph.D. in engineering mechanics from Virginia Polytechnic Institute & State University.

LCO are noted that have stimulated much of the other research on the subject. Next, a summary is provided of the primary physical sources of fluid and structural nonlinearities that can lead to nonlinear aeroelastic response in general and LCO more particularly.

A general account of unsteady aerodynamic models, both linear and nonlinear, is then given before turning to the heart of the paper, which provides a critique of the results obtained to date via various methods using as a framework correlations between theory and experiment or alternative theoretical models. For these correlations, unsteady aerodynamic forces per se, flutter boundaries, and LCOs are each considered in turn. For LCOs, 1) airfoils with stiffness nonlinearities, 2) delta wings with geometrical plate nonlinearities, 3) very high aspect ratio wings with both structural and aerodynamic nonlinearities, 4) nonlinear structural damping, and 5) aerodynamic flows with large shock motions and flow separation are each discussed. A brief mention is also made of recent studies of active control of nonlinear aeroelastic systems.

The authors conclude with a summary of major lessons learned by the research and development community to date and offer a few suggestions for future work that appear particularly attractive at this time.

Generic Nonlinear Aeroelastic Behavior

There are several basic concepts that will be helpful for the reader to keep in mind throughout the discussion to follow. The first is the distinction between a static nonlinearity and a dynamic one. In the aeroelasticity literature the term linear system may either mean a (mathematical or wind-tunnel) model or flight vehicle that is both statically and dynamically linear in its response or one that is nonlinear in its static response, but linear in its dynamic response. Therefore, we will usually qualify the term linear model further by noting whether the system is dynamically linear or both statically and dynamically, that is, wholly, linear.

An example of a system that is wholly linear is a structure whose deformation to either static or dynamic forces is (linearly) proportional to those forces. An aerodynamic flow is wholly linear when the response, for example, change in pressure, is (linearly) proportional to changes in downwash or fluid velocities induced by shape or motion of a solid body in the flow. This is the domain of classical small perturbation aerodynamic theory and leads to a linear mathematical model (convected wave equation) for the fluid pressure perturbation or velocity potential. Shock waves and separated flow are excluded from such flow models that are both statically and dynamically linear. A wholly linear aeroelastic model is of course one composed of wholly linear structural and aerodynamic models.

A statically nonlinear, but dynamically linear, structure is one where the static deformations are sufficiently large that the static response is no longer proportional to the static forces and the responses to the static and dynamic forces cannot simply be added to give meaningful results. Buckled skin panels that dynamically respond to (not too large) acoustic loads or the prediction of the onset of their dynamic aeroelastic instability (flutter) are examples where a statically nonlinear, but dynamically linear model may be useful. (Note that buckling is a nonlinear static equilibrium that arises from a static instability.)

In aerodynamic flows, shock waves and separated flows are themselves the result of a dynamically nonlinear process. However, once formed, they may often be treated in the aeroelastic context as part of a nonlinear static equilibrium state (steady flow). Then the question of the dynamic stability of the statically nonlinear fluid–structural (aeroelastic) system may be addressed by a linear dynamic perturbation analysis about this nonlinear static equilibrium. Often such aerodynamic flow models are call time linearized.

Of course if one wishes to model LCOs and the growth of their amplitude as flow parameters are changed, then either or both the structural and the aerodynamic model must be treated as dynamically nonlinear. Often a single nonlinear mechanism is primarily responsible for the LCO. However, one may not know a priori which nonlinearity is dominant unless one has designed a mathematical model, wind-tunnel model, or flight vehicle with the chosen nonlinearity. Not the least reason why LCOs are more difficult to understand in flight vehicles (compared to, for example, mathematical models) is that rarely has a nonlinearity been chosen and designed into the vehicle. More often one is dealing with an unanticipated and possibly unwanted nonlinearity. Yet sometimes that nonlinearity is welcome because without it the LCO would instead be replaced by catastrophic flutter leading to loss of the flight vehicle.

It must be emphasized that the variety of possible nonlinear aeroelastic response behaviors is not limited to LCOs per se. In the context of nonlinear system theory,[1] an LCO is one of the simplest dynamic bifurcations, a first stop on the road to chaos, so to speak. Other common possible behaviors include higher harmonic and subharmonic resonances, jump resonances, entrainment, beating (which can be due to either linear or nonlinear coupling), and period doubling, to name only a few. These behaviors have been delineated and studied using low-order model problems in the nonlinear dynamics literature; however, in aeroelastic wind-tunnel and flight testing, the detailed knowledge required to identify these nonlinear behaviors has rarely been available. Also, experience indicates that the concept of LCO is a good general description for many nonlinear aeroelastic behaviors. Thus, we will limit ourselves herein to the use of the generic term LCO, acknowledging that this is an oversimplification.

Now let us turn to the generic types of nonlinear dynamic response that may occur, that is, LCOs and the variation of their amplitude with flight speed (or wind-tunnel velocity). Of course, the frequency of the LCO may vary with flight parameters as well, but usually the frequency is near that predicted by a classical linear dynamic stability (flutter) analysis.

The generic possibilities are indicated in Figs. 1a and 1b, where the limit cycle amplitude is plotted vs some system parameter, for example, flight speed. In Fig. 1a, an aeroelastic system is shown
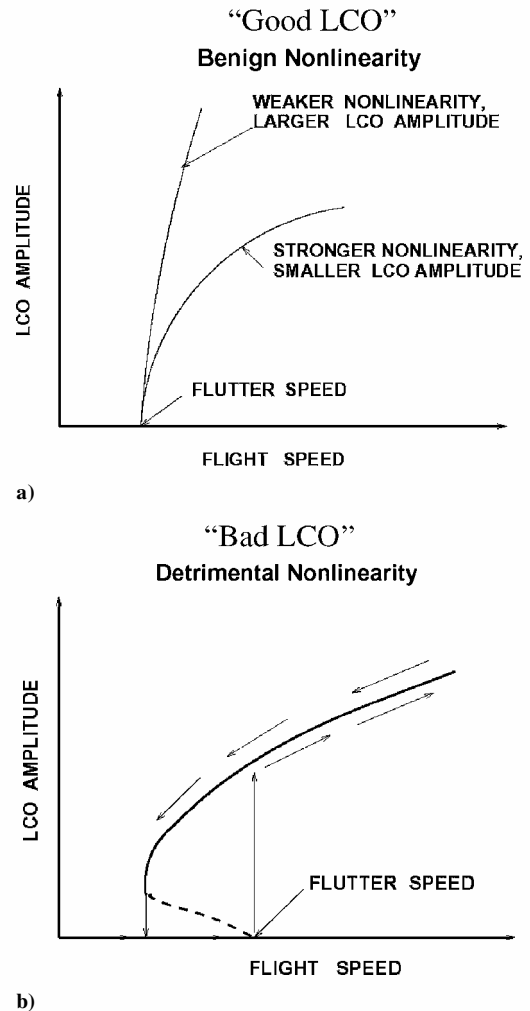

a)

b)

Fig. 1 Schematic of LCO response.

that is stable to small or large disturbances (perturbations) below the flutter (instability) boundary predicted by a linear dynamic model. Beyond the flutter boundary, LCO arise due to some nonlinear effect, and typically the amplitude of the LCO increases as the flight speed increases beyond the flutter speed. In Fig. 1b, the other generic possibility is shown. Whereas again LCOs exist beyond the flutter boundary, now LCOs may also exist below the flutter boundary, if the disturbances to the system are sufficiently large. Moreover both stable (solid line) and unstable (dotted line) LCOs now are present. Stable LCOs exist when for any sufficiently small disturbance, the motion returns to the same LCO at large time. Unstable LCOs are those for which any small perturbation will cause the motion to move away from the unstable LCO and move toward a stable LCO. Theoretically, in the absence of any disturbance, both stable and unstable LCOs are possible dynamic, steady-state motions of the system. Information about the size of the disturbance required to move from one stable LCO to another can also be obtained from data such as shown in Fig. 1b. Note also the hysteretic response as flight speed increases and then decreases.

Flight Experience with Nonlinear Aeroelastic Effects

Much of the flight experience with aircraft LCO has been documented by the Air Force Flight Test Center at Eglin Air Force Base and is described in Refs. 1–5. Most of this work has been in the context of the F-16 aircraft. Denegri distinguishes among three types of LCO based on the phenomenological observations in flight and as informed by classical linear flutter analysis. Typical LCO is when the LCO begins at a certain flight condition and then with, for example, an increase in Mach number at constant altitude, the LCO response smoothly increases. Flutter, as distinct from LCO, is said to occur when the increase in LCO amplitude with change in Mach number is so rapid that the safety of the vehicle is in question. Finally, atypical LCO is said to occur when the LCO amplitude first increases and then decreases and perhaps disappears with changes in Mach number. Often changes in flight vehicle angle of attack lead to similar generic LCO responses to those observed with changes in Mach number.

It has long been recognized[6] that the addition of external stores to aircraft changes the dynamic characteristics and may adversely affect flutter boundaries. LCOs remain a persistent problem on high-performance fighter aircraft with multiple store configurations. Using measurements obtained from flight tests, Bunton and Denegri[7] describe LCO characteristics of the F-16 and F/A-18 aircraft. Although LCO can be present in any sort of nonlinear system, in the context of aeroelasticity, LCO typically is exhibited as an oscillatory torsional response of the wing, the amplitude of which is limited, but dependent on the nature of the nonlinearity as well as flight conditions, such as speed, altitude, and Mach number. The LCO motion is often dominated by antisymmetric modes. LCOs are not described by standard linear aeroelastic analysis, and they may occur at flight conditions below those at which linear instabilities such as flutter are predicted. Although the amplitude of the LCO may be above structural failure limits, more typically the presence of LCOs results in a reduction in vehicle performance, leads to airframe-limiting structural fatigue, and compromises the ability of pilots to perform critical mission-related tasks. When LCO are unacceptable for flight performance, extensive and costly flight tests for aircraft/store certification are required.

Denegri[2] and Denegri and Cutchins[3] suggest that, for the F-16, the frequencies of LCO might be identified by linear flutter analysis; however, linear analysis fails to predict the oscillation amplitude or the onset velocity for LCO. No definitive theory has been forwarded to completely explain the mechanisms responsible for F-16 LCO. Denegri notes that, although linear techniques have been used to predict the frequency of LCOs, linear analysis cannot consistently predict where within the flight envelope the onset of the oscillations will occur. Thus, nonlinear analysis will be necessary to predict the onset of the LCO and their amplitudes with changing flight conditions. Such nonlinear analysis would be a useful and valuable tool for reducing the amount of flight testing necessary for aircraft/store certification.

Nonlinear Aerodynamic Effects

There are several other flight experiences with LCOs in addition to the F-16, including those, for example, with the F-18, the B-1, and B-2. Most of these LCOs have been attributed by a majority of investigators to nonlinear aerodynamic effects due to shock wave motion and/or separated flow. However, there is the possibility that nonlinear structural effects involving stiffness, damping or freeplay may play a role as well. Indeed, much of the present day research and development effort is devoted to clarifying the basic mechanisms responsible for nonlinear flutter and LCO. For an authoritative discussion of these issues see Cunningham,[8,9] Cunningham and Geurts,[10] Denegri,[2] Denegri and Cutchins,[3] Denegri,[4] and Denegri and Johnson[5] on the F-16 and F-18; Dobbs et al.[11] and Hartwich[12] on the B-1; and Dreim et al.[13] on the B-2. Recent experimental evidence from wind-tunnel tests is beginning to shed further light on these matters as are advances in mathematical and computational modeling.

In addition to the preceding studies, many aircraft with freeplay in their control surfaces have experienced LCO as well.

Freeplay

There have been any number of aircraft that have experienced flutter-induced LCOs as a result of control surface freeplay. Not surprisingly, perhaps, these are not well documented in the public literature, but are more known by word of mouth among practitioners and, perhaps, documented in internal company reports and/or restricted government files.

A recent and notable exception is the account by Croft[14] of a flutter/LCO as a result of freeplay. In many ways this account is typical. The oscillation is of limited amplitude, and there was a reported disagreement between the manufacturer and the regulating governmental agency as to whether this oscillation was or was not sufficiently large as to be a threat to the structural integrity of the aircraft structure.

Geometric Structural Nonlinearities

Another not infrequently encountered and documented case is the LCO that follows the onset of flutter in platelike structures. The structure has a nonlinear stiffening as a result of the tension induced by midplane stretching of the plate that arises from its lateral bending. This is most commonly encountered in what is often called panel flutter, where a local element of a wing or fuselage skin encounters flutter and then an LCO. There have been many incidents reported in the literature dating back to the V-2 rocket of World War II, the X-15, the Saturn launch vehicle of the Apollo program and continuing on to the present day. Some of these are discussed by Dowell.[15,16]

It has been recently recognized that low-aspect-ratio wings may behave as structural plates and that the entire wing may undergo a form of platelike flutter and LCOs. This has been seen in both wind-tunnel models and computations to be discussed later in the text. However, there is not yet a clearly documented case of such behavior in flight.

Physical Sources of Nonlinearities

These have been identified through mathematical models (in almost all cases), wind-tunnel tests (in several cases), and flight tests (less often). Among those most commonly studied and thought to be among the more important are the following. Large shock motions may lead to a nonlinear relationship between the motion of the structure and the resulting aerodynamic pressures and forces that act on the structure. If the flow is separated (perhaps in part induced by the shock motion), this may also create a nonlinear relationship between structural motion and the consequent aerodynamic flowfield.

Structural nonlinearities can also be important and are the result of a given (aerodynamic) force on the structure creating a response that is no longer (linearly) proportional to the applied force. Freeplay and geometric nonlinearities are prime examples (already mentioned). However, the internal damping forces in a structure may also have a nonlinear relationship to structural motion, with dry friction being

an example that has received limited attention to date. Because the structural damping is usually represented empirically even within the framework of linear aeroelastic mathematical models, not much is known about the fundamental mechanisms of damping and their impact on flutter and LCO.

All of these nonlinear mechanisms have, nevertheless, been considered by the mathematical modeling community, and several have been the subject of wind-tunnel tests as well. In some cases good correlation between theory and experiment has been obtained for LCO response.

Efficient Computation of Unsteady Aerodynamic Forces: Linear and Nonlinear

The literature on unsteady aerodynamic forces alone is quite extensive. A comprehensive assessment of current practice in industry is given by Yurkovich et al.[17] An article that focuses on recent developments is that of Dowell and Hall.[18] They also developed a bibliography of some 500 items available in electronic form from the authors. Other recent and notable discussions include those of Bennett and Edwards[19] and Beran and Silva.[20] Much of the present focus of work on unsteady aerodynamics is on developing accurate and efficient computational models. Standard computational fluid dynamic (CFD) models that include the relevant fluid nonlinearities are simply too expensive now and for some time to come for most aeroelastic analyses. Thus, there has been much interest in reducing computational costs while retaining the essence of the nonlinear flow phenomena.

There are three basic ideas that are currently being pursued with some success in retaining the accuracy associated with state-of-the-art CFD models while reducing aerodynamic model size and computational cost.[18,20] One is to consider a small (linear) dynamic perturbation about a (nonlinear) mean steady flow. The steady flow may include both the effects of a shock wave and flow separation, but any shock or flow separation region motion is considered in the dynamically linear approximation. That is, it is assumed that the shock motion or the separation point motion, for example, is linearly proportional to the motion of the structure. This is sufficient to assess the linear stability of the aeroelastic system, but not to determine LCO amplitudes due to nonlinear aerodynamic effects. Of course, in those cases where the structural nonlinearities are dominant, this simpler aerodynamic model is all one needs to determine LCO. This approach has enormous computational advantages because the computational cost is comparable to that of a steady flow CFD model because the unsteady calculation per se uses a linear model. Although this time linearization approach can be employed in either the time or frequency domain, usually it is most efficient to do the calculation in the frequency domain. The time linearization combined with the frequency-domain aeroelastic calculation is several orders of magnitude faster than a time-marching nonlinear CFD method for the determining the flutter boundary without any loss of accuracy for this purpose. Also if a parameter study is conducted where only the structural parameters are varied, then the additional computational cost is no more than that using classical aerodynamic methods.

Moreover this approach can be extended to nonlinear unsteady flows by expanding the flow solution in terms of a Fourier series in time. This assumes the flow motion is periodic in time, of course, and is most effective if the number of important harmonics needed in the Fourier series is small. However, this is true of many (but not all) flows of interest. Here the computational cost is a small multiple, for example, a factor of three, of the cost of a steady flow solution. This is the second major idea, and again the harmonic balance method is much faster for determining the LCO than a time marching of a nonlinear CFD code, typically by one or two orders of magnitude.

The third major idea is to determine the dominant spatial modes of the flowfield and use these, rather than many local grid points, to represent the flow. This is a class of so-called reduced order models. The reduction is from the very large number of local grid points (on the order of a million or more) to a small number of spatial modes (typically less than 100). The reduction in computational cost for aeroelastic analysis is several orders of magnitude, that is, a factor of 1000 or more. This approach has been used for potential flow, Euler flow, and Navier–Stokes flows (with a turbulence model) for small dynamic perturbations about a nonlinear mean steady flow. (Recall the first major idea discussed earlier.) Current research is underway to consider nonlinear unsteady flows. Kim and Bussoletti[21] have discussed how one can construct an optimal reduced-order aeroelastic model within the framework of time-linearized CFD models. Whereas in principal fluid eigenmodes can be used and indeed they provide the underlying framework for reduced-order modeling, the technique known as proper orthogonal decomposition has proven to be the most computationally attractive method for constructing a set of global modes for the reduced order model. With a reduced order model (ROM), the aeroelastic computations are essentially at no additional cost beyond the construction of the ROM itself. To say it another way, the aeroelastic computations are no more expensive than using a classical unsteady aerodynamics. Moreover, one can construct a root locus solution for the true aeroelastic eigenvalues (true damping and frequency of each aeroelastic mode).

A parallel approach to the last idea is to use the ideas of transfer functions (sometimes called describing functions in the nonlinear case) in the frequency domain or Volterra series in the time domain to create small computational models from large CFD codes. In this approach, the form of the transfer function or describing function (or its time series equivalent) is assumed, and the coefficients of the ROM are determined from data generated by the CFD code in a time simulation. A good discussion of this approach is found by Beran and Silva[20] and in a series of papers by Silva.[22−27] Again this approach is most fully developed for the dynamically linear case, and the dynamically nonlinear case is currently a subject of active research. Raveh et al.[28] have offered a recent and useful discussion of how these ideas can be implemented within the framework of an Euler-based, CFD model and provided an example of the well-studied AGARD 445.6 wing. Also see Raveh.[29]

All of these ideas, individually or in combination, provide the promise of dramatic reductions in computational costs for unsteady transonic flows including the effects of shock motion and flow separation. In addition, progress continues to be made in improving the computational efficiency of time-marching simulations.[30,31] Also the ideas of dynamic (time) linearization and reduced order modeling can be used in either the time or frequency domains.

Experimental/Theoretical and Theoretical/ Theoretical Correlations

Much of what we know about the state of the art with respect to nonlinear aeroelasticity comes from the study of correlations between experiment and theory and between various levels of theoretical models. Hence, the remainder of this paper is largely devoted to such correlations and the lessons learned from them. The correlations selected are, to the best of our knowledge, representative of the state of the art. We shall consider correlations for aerodynamic forces per se, transonic flutter boundaries, and LCOs.

Aerodynamic Forces

Roughen et al.[32] have compared the results of several theoretical models with the experimental data from the Benchmark Active Controls Technology (BACT) wing. The BACT wing is a rectangular planform with a NACA 0012 airfoil profile. The model has a trailing-edge control surface extending from 45 to 75% span. Previously, Schuster et al.[33] had compared results from a Navier–Stokes CFD model (ENS3DAE) to these experimental data. Roughen et al.[32] used an alternative Navier–Stokes CFD model (CFL3D) and also a classical potential flow model (doublet lattice). Correlations were made at several subsonic to transonic Mach numbers. They observe:

> For the purely subsonic condition [$M = 0.65$]... there is relatively good agreement between the doublet-lattice results, the Navier–Stokes results and the test data. This is not surprising because the flow is entirely subsonic and well behaved [there is no shock wave and no flow separation]. [However at $M = 0.77$] transonic effects begin to become apparent in these results. For the most part, the observations about the results and the qualitative correlation between doublet lattice, Navier–Stokes, and experimental
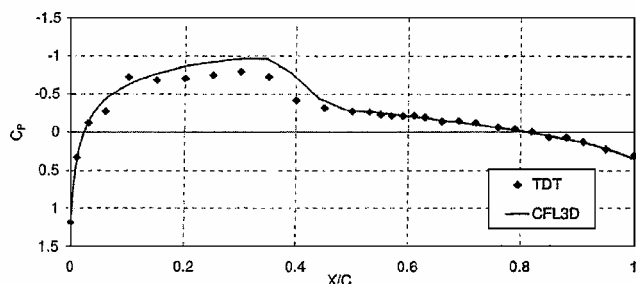
Fig. 2   Steady-state pressure distribution for BACT model.

results are similar to the subsonic results. However, there are some important differences that appear in the neighborhood of the super-sonic pocket [near the mild and relatively weak shock wave]. . . . There is clearly a bump in the unsteady pressure magnitude [near the shock wave position]. . . . Little nonlinear amplitude dependence is seen [however] except near the trailing edge.

For $M = 0.82$, there is a strong shock near 40% chord. "The presence of the shock is also clearly evident in the steady-state pressure distribution shown in Fig. 2. The effects of the shock are also quite obvious in the unsteady pressure results (Fig. 3). In the unsteady pressure magnitudes, there is a clear peak in the unsteady pressure at approximately 35% local chord in the experimental results and at 40% local chord in the Navier–Stokes results. The peak, which represents the shock doublet[34] caused by the unsteady motion of the shock, is absent in the linear doublet lattice results (N5K code). Quantitatively, the correlation of the shock doublet peak between experimental and Navier–Stokes results is disappointing. The CFD results predict a shock doublet of approximately double the amplitude of that seen in the experimental results. . . . Possible contributors to this inaccuracy (in the theory) are the chordwise grid resolution and the Baldwin–Lomax turbulence model. Correlation between CFD solutions and the experiment is excellent away. . . from the shock."

Another valuable correlation among several theoretical results and that of experiment is based on the experimental work of Davis and Malcolm.[35] Several investigators have compared the results of transonic potential flow and Euler flow models with these experimental data. See Dowell and Hall[18] for citations to and discussion of original references. A NACA 64A010A airfoil was studied, again in the high subsonic/transonic Mach number range. See Figs. 4a–4d for a comparison of lift and moment magnitude and phase for a pitching airfoil. As can be seen, the general trends are well predicted by all theories with the Euler model being in somewhat better agreement with the experimental data overall. The most recent Euler results were obtained using the harmonic balance method, and the number of data points calculated were correspondingly more numerous. For this comparison, the mean angle of attack of the airfoil was a 0 deg. However, Davis and Malcolm[35] also considered a mean angle of attack of 4 deg for which the flow is separated, and results for the magnitude of the unsteady lift are shown in Fig. 5 for both mean angles of attack as a function of the amplitude of the oscillating or unsteady angle of attack. What is immediately clear is that for the mean angle of attack of zero there is a significant range of unsteady angle of attack for which the aerodynamic flow is dynamically linear. However, that range is much smaller when the mean angle of attack is increased to 4 deg and the flow is separated. Results from both potential flow and Euler flow models correlate well with the experiment for a mean angle of attack of 0 deg when the flow is attached, but not for the case of a mean angle of attack of 4 deg when the flow is separated. It would be very valuable to have results from a Navier–Stokes model for the latter case. McMullen et al.[36] have also done calculations for this set of experimental data using the harmonic balance method and obtained similar results. They have done a careful grid convergence study as well.

Finally the valuable study of Kreiselmaier and Laschka[37] is noted. In this work, they develop a time-linearized Euler model and compare the results obtained to those from a fully dynamically nonlinear Euler model. The cases considered are a NACA 0012 airfoil in subsonic flow, the NACA 64A010 in transonic flow, and a 3% parabolic

arc airfoil in supersonic flow, as well as the three-dimensional flow about the LANN wing. Their principal conclusions are that the computational cost of the time-linearized code is about an order of magnitude less than that of the fully nonlinear code (consistent with the findings of other investigators) and that the results from the two theoretical models are in good agreement for the cases and parameter ranges investigated. As already noted, a time-linearized flow model is sufficient to predict the flutter boundary per se, but of course cannot predict LCO amplitudes.

A recent NATO report by a Research and Technology Organization Working Group (Ruiz-Calavera[38]) provides a comprehensive experimental database drawn from many sources in the literature for the verification and validation of computational unsteady aerodynamic computational codes. Comparisons of the experimental data with selected aerodynamic computer models and codes are also provided. Additional theoretical/experimental correlations may be expected using this unique collection of data.

Flutter Boundaries in Transonic Flow

Bennett and Edwards[19] have discussed the state of the art of computational aeroelasticity (CAE) in a relatively recent paper and made several insightful comments about various correlation studies. The NASA Langley Research Center team pioneered in providing correlations for the AGARD 445.6 wing in the transonic flow region. In Figs. 6a and 6b comparison between the results of experiment and theory is shown for flutter speed index (FSI) and flutter frequency as functions of Mach number. The theoretical results are for transonic nonlinear potential flow theory without (CAP-TSD) and with (CAP-TSDV) a boundary-layer model to account for viscous flow effects and also for an Euler (CFL3D-Euler) and a Navier–Stokes (CFL3D-NS) flow model. For this thin wing, there are no significant transonic effects in the steady flow over the wing surface at the Mach numbers with experimental results except for $M = 0.96$, where there is a very weak shock on the surface. For the subsonic conditions, all computational results are in very good agreement with experiment. The two low supersonic test conditions have been problematic for CAE. Inviscid computations have produced high FSI values relative to the experimental FSI, and viscous computations have accounted for about one-half the difference between theory and experiment. Several investigators have now done similar Euler calculations and obtained similar results.[39−41] The excellent agreement of the wholly linear theory results with experiment should probably be regarded as fortuitous. Interestingly, Gupta,[42] who also used an Euler-based CFD model, obtains results in better agreement with experiment at the low supersonic conditions, though in less good agreement with experiment than the other Euler-based results at subsonic conditions. Thus, CAE computations for this low supersonic region have unresolved issues, which probably involve details such as wind-tunnel wall interference effects and flutter test procedures, as well as CAE modeling issues.

High-Speed Civil Transport Rigid and Flexible Semispan Models

Two semispan models representative of high-speed civil transport (HSCT) configurations were tested in the NASA Langley Research Center Transonic Dynamics Tunnel (TDT) in heavy gas. A rigid semispan model (RSM) was tested mounted on an oscillating turntable (OTT) and on a pitch and plunge apparatus (PAPA). The RSM/OTT test[43] acquired unsteady pressure data due to pitching oscillations and the RSM/PAPA test acquired flutter boundary data for simple pitching and plunging motions. The RSM test[44] involved an aeroelastically scaled model and was mounted to the TDT sidewall. The test acquired unsteady pressure data and flutter boundary data. Figure 7 (Ref. 43) shows the unexpectedly large effect of mean angle of attack on the flutter boundaries for the RSM/PAPA model. Flutter of thin wings at subsonic conditions is typically independent of angle of attack within the linear flow region. Figure 8 (Ref. 42) shows a summary of the flutter and high dynamic response regions for the RSM. Squares indicate conditions where forced response measurements due to trailing edge control surface oscillations were made. The analysis flutter boundary is from an early finite element model. Updated modeling places the (linear) flutter boundary slightly above
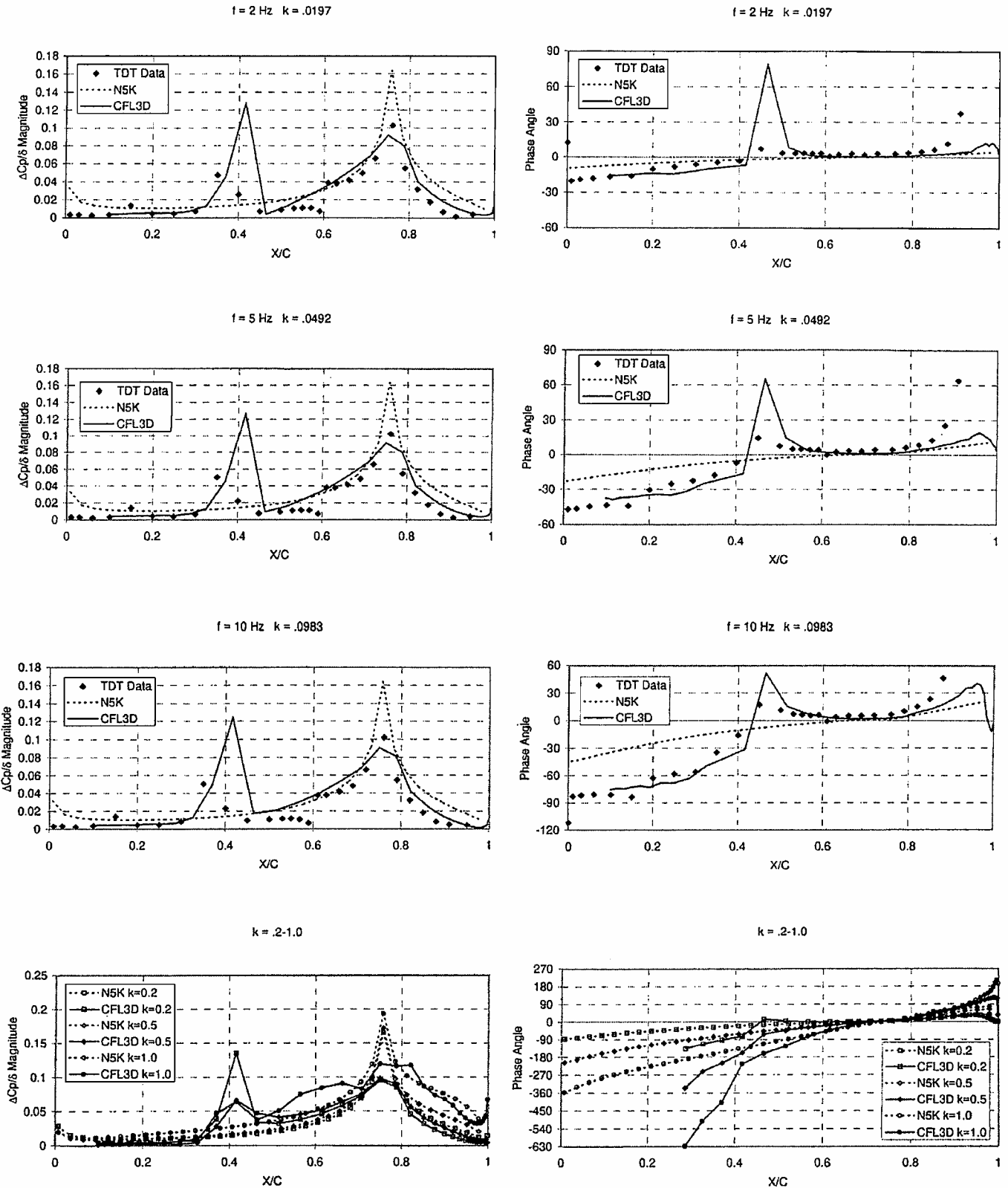
Fig. 3 Unsteady pressure distributions of BACT model analysis at 60% span station, $M = 0.82$, $\alpha = 0$ deg, and flap deflection = 4 deg.

the indicated hard flutter point. A region of increased response in first wing bending (8.5 Hz) was encountered in the Mach number range of 0.90–0.98. Finally, a narrow region of LCO behavior, labeled chimney, was encountered for $M = 0.98$–1.00 and over a wide range of dynamic pressures. Response frequency ranged from 11.9 to 14.0 Hz, and the region was traversed a number of times before encountering the hard flutter point at $M = 0.979$ and $q = 246$ psf or 11.8 kPa where the model was lost.

BACT Model

This rectangular wing model had a panel aspect ratio of two and a NACA 0012 airfoil section.[45−47] It was mounted on a PAPA, which allowed flutter testing with two simple degrees of freedom. It was extensively instrumented with unsteady pressure sensors and accelerometers, and it could be held fixed (static) for forced oscillation testing or free for dynamic response measurements. Data sets for trailing-edge control surface oscillations and upper-surface spoiler
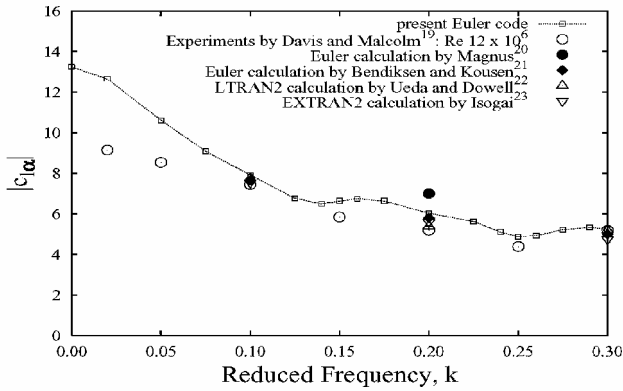
Fig. 4a   Lift magnitude due to pitching ±1 deg at the quarter chord for $M = 0.8$ vs reduced frequency $k \equiv \omega b/U_\infty$. See Dowell and Hall[18] for citations to original literature.
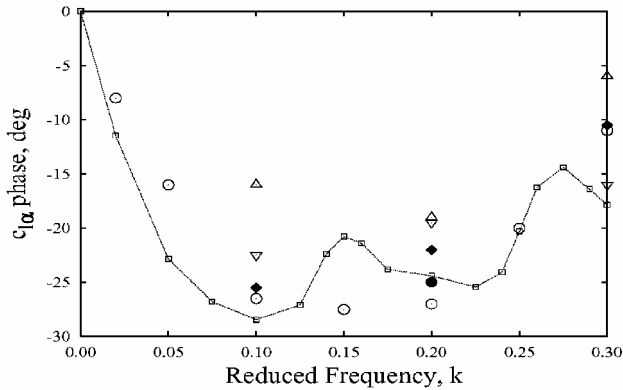

Fig. 4b   Lift phase due to pitching ±1 deg at the quarter chord for $M = 0.8$ vs reduced frequency $k \equiv \omega b/U_\infty$.
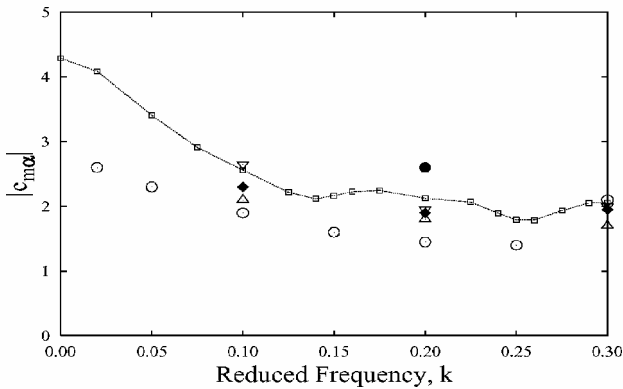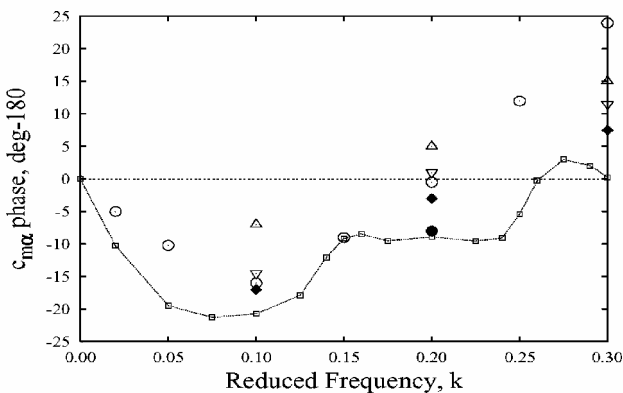

Fig. 4c   Leading-edge moment magnitude due to pitching ±1 deg at the quarter chord for $M = 0.8$ vs reduced frequency $k \equiv \omega b/U_\infty$.

Fig. 4d   Leading-edge moment phase due to pitching ±1 deg at the quarter chord for $M = 0.8$ vs reduced frequency $k \equiv \omega b/U_\infty$.
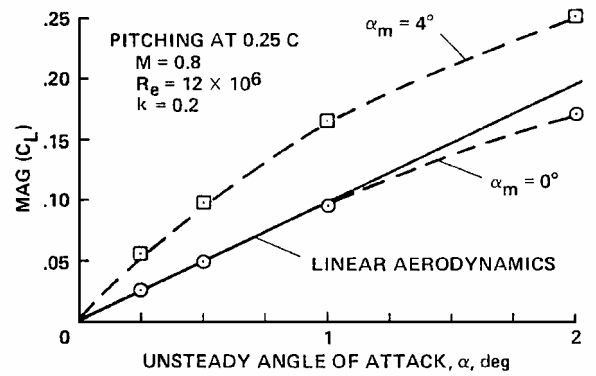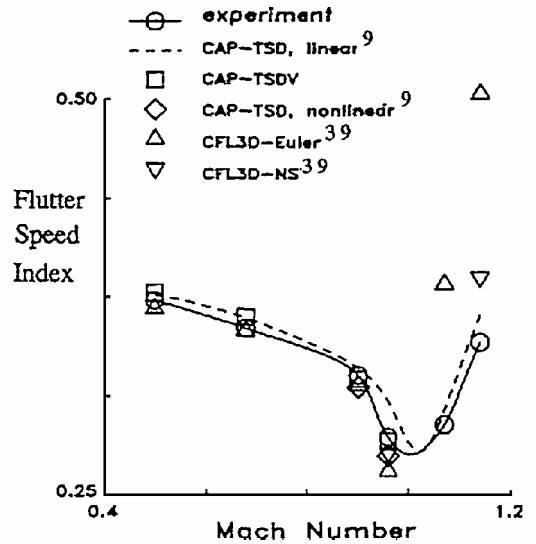

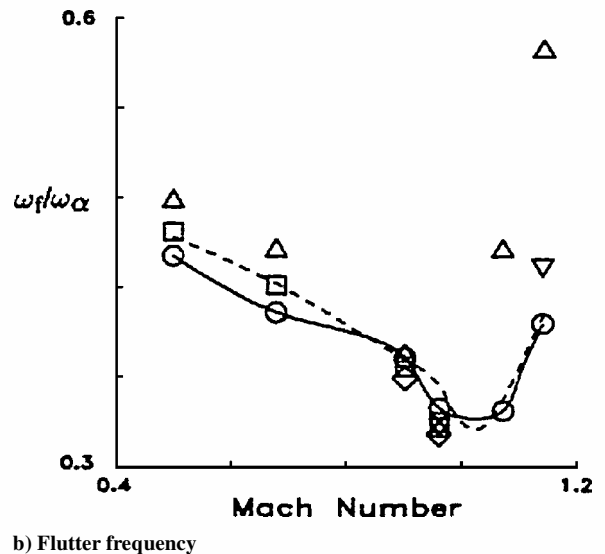**Fig. 5   Unsteady lift magnitude vs unsteady angle-of-attack magnitude.**

a) FSI

b) Flutter frequency

Fig. 6   FSI and flutter frequency vs Mach number for AGARD 445.6 wing.

oscillations for a range of Mach numbers, angle of attack, and static control deflections are available. The model exhibited three types of flutter instability illustrated in Fig. 9.

A classical flutter boundary is shown, for $\alpha = 2$ deg, as a conventional boundary vs Mach number with a minimum, the transonic dip, near $M = 0.77$ and a subsequent rise. Stall flutter was found, for $\alpha > 4$ deg, near the minimum of the flutter boundary (and at most tunnel conditions where high angles of attack could be attained).
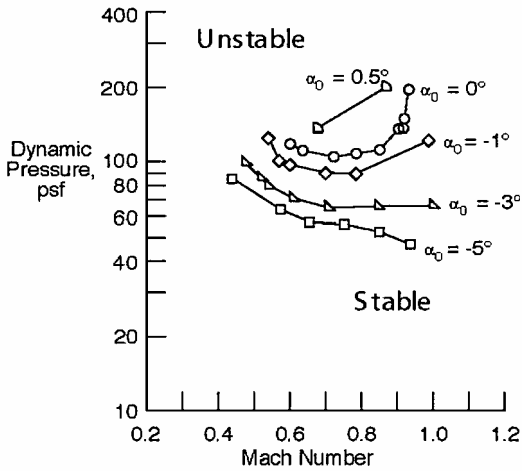
Fig. 7   Flutter dynamic pressure vs Mach number for various mean angles of attack.
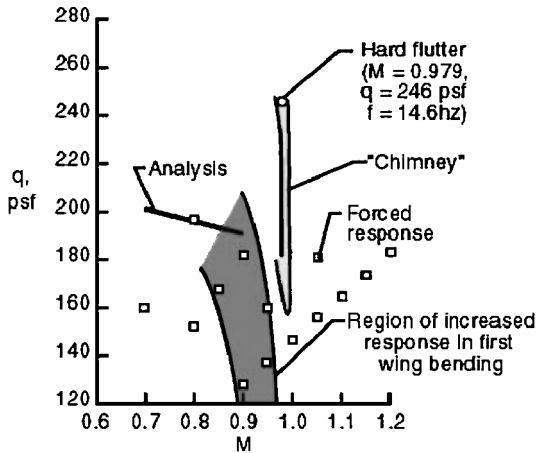

Fig. 8   Dynamic pressure vs Mach number: regions of distinct response for HSCT model.
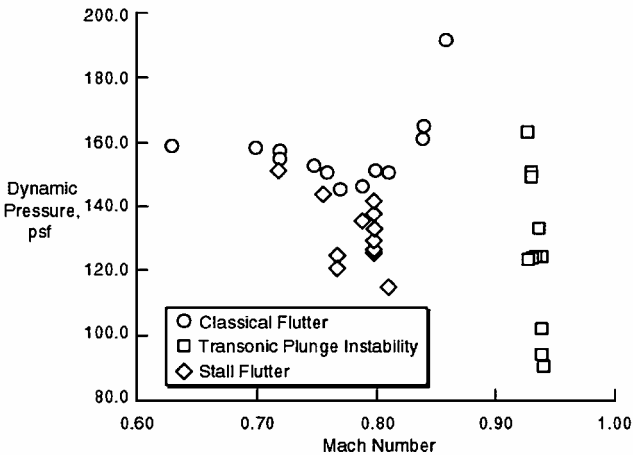

Fig. 9   Dynamic pressure vs Mach number: regions of distinct response for BACT model.

Finally, a narrow region of instability occurs near $M = 0.92$, consisting of plunging motion at the plunge mode wind-off frequency. This type of transonic instability has sometimes been termed single-degree-of-freedom flutter. It is caused by the fore and aft motion of symmetric shocks on the upper and lower surfaces for this wing. It was very sensitive to any biases and does not occur with nonzero control surface bias or nonzero alpha. Such a stability boundary feature is sometimes termed a chimney because the oscillations are typically slowly diverging or constant amplitude (LCO), and it is found, sometimes, that safe conditions can be attained with small

further increases in Mach number. Note that the Mach number for the plunge instability decreases slightly with increasing pressure. Bartels and Schuster[47] compare Reynolds averaged Navier–Stokes (RANS) code computations of some BACT model forced oscillation responses with experimental data.

Isogai[48] Case A Model

Another benchmark case often used for theoretical/theoretical comparisons is the famous Isogai[48] case A, again for a NACA 64A010 airfoil with certain structural parameters that lead to a complex transonic flutter boundary for a plunging and pitching airfoil. A recent study is that by Hall et al.[49,50] that includes comparisons with the earlier results of Isogai,[48] Ehlers and Weatherill,[51] and Edwards et al.[52] The latter results were all obtained using nonlinear potential flow models. (In some cases they were time linearized, which should make no difference for determining the flutter boundary per se.), However, the results of Hall et al.[49,50] were obtained using a time-linearized Euler model. There is encouraging agreement among all models for this complex transonic flutter boundary, as seen in Fig. 10. Note the rapid change in FSI as the Mach number is varied. This is associated with a change in the critical flutter mode (eigenvector). Two additional studies, Prananta et al.[53] and Bohbot and Darracq,[54] have included turbulence modeling for this case. Their results show that viscosity reduces the extent of the transonic dip in the flutter boundary significantly and eliminates the double-valued FSI that are seen over a portion of the Mach number range in the inviscid calculations. Bohbot and Darracq[54] also show a significant decrease in LCO amplitude due to viscosity at $M = 0.9025$.

Bendiksen[55−57] has made two important observations about transonic flutter boundaries. One is with respect to an experimental study done some years ago at NASA Langley Research Center to consider the effects of airfoil thickness ratio from Dogget et al.[58] for the same airfoil profile. Bendiksen notes that the family of results for the variation of flutter speed index with Mach number for the several thickness ratios can be reduced to a single curve when the data are replotted using classical (nonlinear potential flow) transonic steady flow similarity variables. These similarity parameters rescale the aerodynamic pressure using nondimensional parameters that combine the Mach number and thickness ratio. Essentially this rescaling shows an equivalence between changes in Mach number and thickness ratio in the transonic range. Because the rescaling is based on steady flow similarity variables, it presumably works best when the reduced frequency is small as might be the case for bending/torsion flutter, but perhaps not for single-degree-of-freedom flutter due to negative damping. See, for example, Dowell et al.[59] for a discussion of various types of flutter that may occur. Implicitly the success of this rescaling also supports the more general
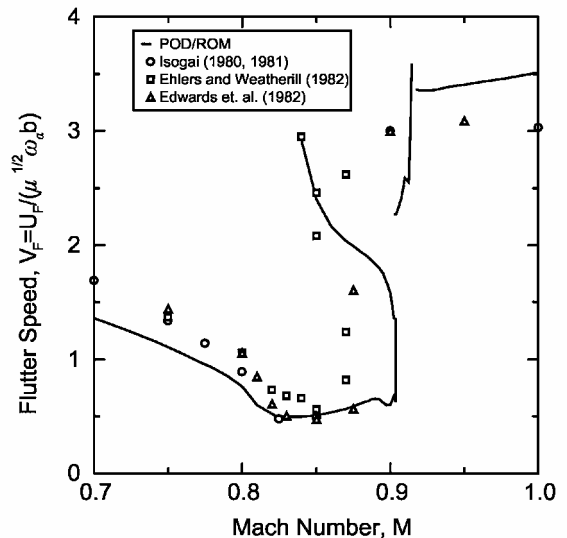

Fig. 10   FSI vs Mach number for Isogai[48] case A.

observation that for transonic flow it is important to model accurately the position and strength of the shock wave for steady flow conditions before attempting unsteady aerodynamic or aeroelastic calculations.

The other important point made by Bendiksen is that in the transonic range the FSI may vary rapidly, not only because of a change in flutter type or mode (as has been noted by several investigators), but also because of the substantial changes in mass ratio that may occur in wind-tunnel test trajectories. This may explain in part the chimneys in flutter boundaries that have been observed in transonic flutter wind-tunnel test data.

In this regard, note that Denegri[2] presents flight-test data showing LCO at nearly constant Mach number over large variations of altitude. Many typical LCO encounters result in termination of testing due to increasing response levels with each increase in Mach number because of concern for aircraft safety. Some nontypical LCO encounters are reminiscent of the chimney feature in that response levels increased to a maximum and then decreased with increasing Mach number.

LCOs

Airfoils with Stiffness Nonlinearities

Many investigators have considered such a configuration with a variety of nonlinear stiffness modes. For a description of the work on freeplay nonlinearities including a discussion of the literature, see Dowell and Tang,[60] where the focus is on correlations between theory and experiment. In general good quantitative correlation is found for simple wind-tunnel models, and the basic physical mechanism that leads to LCO appears well understood. Among the important insights developed include the demonstration that the LCO amplitude and the effect of mean angle of attack on LCO amplitude both simply scale in proportion to the range of freeplay present in the aeroelastic system.

Next we consider in more depth the valuable and recent work in Refs. 61–66. The authors have conducted experiments with their nonlinear aeroelastic test apparatus (NATA) in a low-speed wind tunnel, and these investigations of typical section models provided validation of their theoretical models (Fig. 11). The NATA testbed has been used to investigate both linear and nonlinear responses of wing sections, as well as the development of active control methods. Three wing sections have been used in their research: a NACA 0015 wing section without a control surface, a NACA 0015 wing section with a 20% chord full-span trailing-edge control surface, and a NACA 0012 wing section with a 15% chord, full-span leading edge and a 20% chord, full-span trailing-edge control surfaces. The pitch and plunge stiffness of the NATA is provided by springs attached to cams with shapes prescribed to impart specific response. For example, a parabolic pitch cam yields a spring hardening response tailored to mimic the response of interest. With such a nonlinear pitch cam in place, the system will experience LCO response. Note that similar nonlinear spring hardening behavior has been observed in static measurements of the F/A-18 wing.[66] A polynomial representation of the spring hardening behavior provides a quite

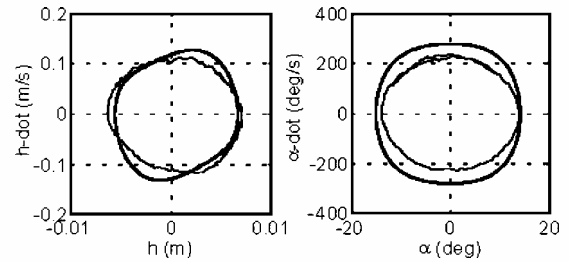**Fig. 11   NATA in the Texas A&M University 2ft × 3ft wind tunnel.**

Fig. 12   Large amplitude LCOs, induced by a hardening in structural stiffness, measured with NATA: ——, measured and ▬, predicted.

effective model of the response. Encoders are use to measure all motions.

The experimental and analytical efforts of O'Neil et al.[61] used a model with a nonlinear structural stiffness. In these studies, the stiffness grew, that is, spring hardened, in a smooth, continuous manner with amplitude of motion. The effect on flutter of a structure with stiffness that grew in a cubic manner was investigated, and the results showed that LCOs occurred and the stability boundary was insensitive to initial conditions. As the freestream velocity was increased, the amplitude of the LCO increased, and less time was required to reach the LCO. A representative result for LCO shown as phase plane diagrams is presented in Fig. 12.

Nonlinear Internal Resonance Behavior

Unusual findings from a wind-tunnel experiment have been a motivation for studies of the possible presence of internal resonances in aeroelastic systems. Internal resonance (IR) occurs as a result of nonlinearities present in the system and leads to an exchange of energy between the system modes. The amount of energy that is exchanged depends on the type of nonlinearity and the relationship of the linear natural frequencies. IR exists when the linear natural frequencies of a system are commensurable, or nearly so, and the nonlinearities of the system provide a source of coupling. Although an integer natural frequency ratio does not guarantee IR, it does form a necessary condition for IR. IR has been shown to exist in many systems, and its presence depends on the geometry, composition of nonlinearities, and boundary conditions.

During wind-tunnel tests by Cole[67] intended to verify the aeroelastic stability of a new wing design, an unexpected flutter-type response occurred at dynamic pressures much lower than analysis had predicted. Note that predictive tools based on linear theory were used. For the physical structure, the natural frequency of the second bending mode of the wind-tunnel model was slightly more than twice the natural frequency of the first torsional mode. However, because frequencies in an aeroelastic system depend on the aerodynamic loads, a system's frequencies may be tuned as the velocity changes. In Cole's experiments, a resonance-type condition may have been reached before linear flutter conditions. Consequently, it was considered that the inaccurate predictions were due to the limitations presented by the use of linear theory.

In an attempt to explain the unexpected experimental results, Oh et al.[68] developed an experiment to examine the structural dynamic behavior of Cole's experiments.[67] These experiments were conducted in the absence of any aerodynamic loads. They[68] determined, theoretically and experimentally, the linear natural frequencies and the mode shapes, and also experimentally showed that an antisymmetric vibration mode of a cantilever metallic plate was indirectly excited by a 2:1 IR mechanism. To explain the experimental results, they referred to the study of Pai and Nayfeh,[69] in which they considered nonlinear beam theory. The two-to-one IR was present because the natural frequency of the second bending mode was nearly twice the natural frequency of the first torsional mode. Their experiment consisted of a base excitation being applied to a cantilevered plate with the same aspect ratio as Cole's[67] wing. However, in this study[69] the second bending mode was excited by a shaker rather than by aerodynamic forces.

IR has been used to suppress the vibrations of flexible structures. Studies show that, during the resonance, the nonlinear modal
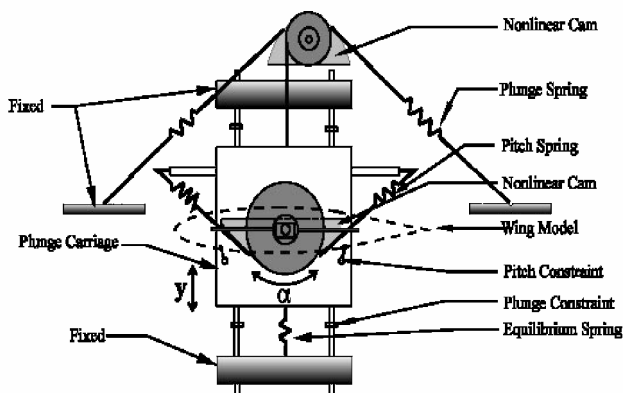
amplitudes exchanged energy back and forth over time, even in the presence of damping. It was also shown that in the presence of an external excitation, the IRs give rise to coupling between the modes, leading to several motions including nonlinear periodic, almost periodic, and chaos.

Although many researchers have investigated IR in various types of mechanical systems, relatively little attention has been given to the study of IR in aeroelastic systems. Stearman et al.[70] studied resonances in aeroelastic systems and showed that both combination-type and parametric resonances can occur. These resonances occurred if

$$\Omega_f \approx 2\omega_n/k, \qquad \Omega_f \approx |\omega_i \pm \omega_j|/k$$

where k is an integer, Ω_f is the frequency of the external forcing function, and ω_i, ω_j, and ω_n are normal mode frequencies. Their study explored the use of statistical techniques to analyze flight-test data.

Gilliatt et al.[71] and Chang et al.[72] studied the possible presence and effects of internal resonances in aeroelastic systems. Gilliatt et al.[71] in particular, were motivated by the experimental findings of Cole.[67] The two-degree-of-freedom model of the O'Neil et al.[61] research was a basis for the study, and a quasi-steady aerodynamic model was extended to include stall effects, which introduced strong cubic nonlinearities into the equations of motion. The system parameters were selected to permit the aeroelastic frequencies to pass through a 3:1, 2:1, and 1:1 ratio as the flowfield velocity was increased. Gilliatt et al.[71] found that the presence of cubic nonlinearities in the aeroelastic system led to a 3:1 IR.

Delta Wings with Geometrical Plate Nonlinearities

At low Mach numbers, good correlation has been demonstrated between theory and experiment for LCO amplitudes and frequencies. Because these results are well documented elsewhere (Dowell and Tang[60]), here the recent work of Gordnier and Melville[73,74] that has extended these correlations into the transonic range is emphasized. In Fig. 13 a cropped delta wing planform is shown. This configuration had been investigated experimentally by Schairer and Hand,[75] and the theoretical calculations were done by Gordnier and Melville[73,74] using both Euler and Navier–Stokes flow models. Initially the theoretical calculations were done using a linear structural model, which gave predicted LCO amplitudes much greater than those observed experimentally. This led Gordnier and Melville to include nonlinearities in the structural model via von Kármán's nonlinear plate theory that provided much improved correlation between theory and experiment. See Fig. 14, which shows LCO amplitude vs flow dynamic pressure at a fixed transonic Mach number. Note that the effects of viscosity are modest, based on the comparisons of results using the Euler vs Navier–Stokes models. Also the much improved agreement obtained with the nonlinear structural model suggests that aerodynamic nonlinearities per se are not as significant for this configuration as are the structural nonlinearities, as Gordnier and Melville note in their conclusions. Perhaps the most significant impact of this example is to illustrate that, even for a transonic flow, there are cases where structural nonlinearities may be dominant.

Note that for this example the most significant aerodynamic nonlinearity was associated with leading-edge vortices rather than
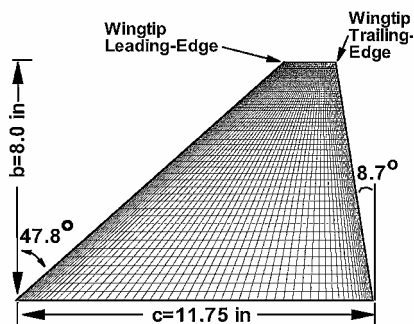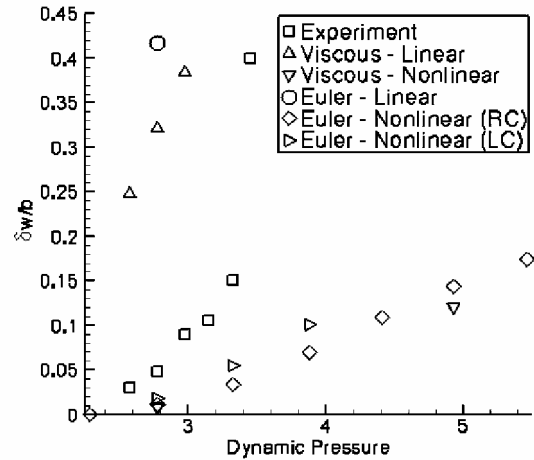
Fig. 14 LCO response vs dynamic pressure: correlation of experiment with various theoretical models for cropped delta wing.

shock motion. This nonlinear aerodynamic flow mechanism has also been studied by Preidikman and Mook[76] at low Mach numbers. As Gordnier and Melville[73,74] and Preidikman and Mook[76] note, nonlinear vortex flow phenomena may be important when structural nonlinearities are weaker and the corresponding structural motions greater. Of course, if the mean angle of attack is sufficiently large, for example, 10 deg or more, then vortex formation may be important for even smaller wing oscillations.

Very High Aspect Ratio Wings with Both Structural and Aerodynamic Nonlinearities

Notable contributions have been made by Patil et al.[77,78] and Tang and Dowell.[79,80] This case has been discussed in some depth by Dowell and Tang,[60] and that discussion will not be repeated here. In summary, however, both structural geometrical nonlinearities (associated with torsional motion and bending both transverse and parallel to the beam/rod chord) and aerodynamic nonlinearities (associated with flow separation and wing stall) have been shown to be important. Also wing stall has been shown to lead to hysteretic LCO response with increases and decreases in flow velocity. The correlation of theory and experiment is good,[79,80] albeit the extant theory uses a semi-empirical model to account for wing stall. Again it would be highly desirable to use a Navier–Stokes flow model for correlation with this experiment, and indeed this case is a good benchmark for such flow models.

Further recent work has been done by Kim and Strganac,[81] who used the structural model of Crespo da Silva and Glynn[82] to examine store-induced LCOs for the cantilevered wing-with-store configuration. This model contains structural coupling terms and quadratic and cubic nonlinearities due to curvature and inertia. Several possible nonlinearities, including aerodynamic, structural, and store-induced sources, were considered. Structural nonlinearities were derived from a large deformation theory. Aerodynamic nonlinearities were introduced through a stall model. Store-induced nonlinearities were introduced by kinematics of a suspended store. All of these nonlinearities retained cubic nonlinear terms. To examine systematically the response characteristics, phase plane analysis was performed, and the effects of each nonlinearity, as well as combinations of the nonlinearities, were studied. Although various forms of nonlinear responses were found, of interest was the finding of LCO response at speeds below the flutter velocity. Furthermore, an unstable boundary was found, above which responses were attracted to the LCO and below which the responses were attracted to the nominal static equilibria. Of special importance, such subcritical response was found for only the case in which complete consideration of structural, aerodynamic, and store-induced nonlinearities was given. This suggested that studies of nonlinear aeroelasticity must sometimes consider a full aircraft configuration. A representative result is shown in Fig. 15.
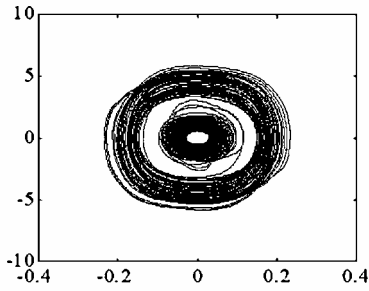
Fig. 13 Planform of a cropped delta wing.

Fig. 15   LCO response of cantilevered wing-with-store configuration.
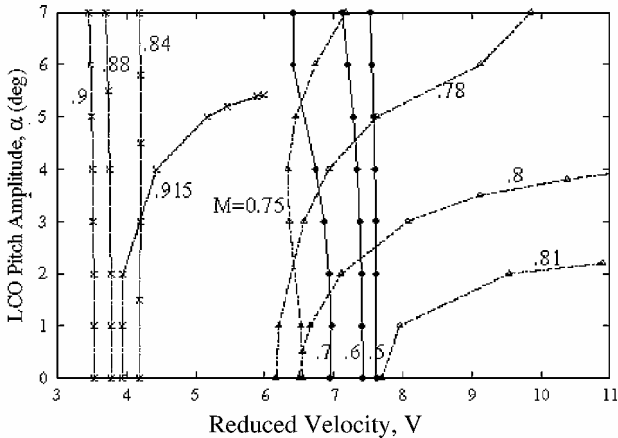

Fig. 16   LCO amplitude vs reduced velocity for NACA 64A010 airfoil.

Thompson and Stragnac[66] studied the effects of structural nonlinearities and store configuration nonlinearity. Thompson and Stragnac showed that although store-induced kinematic nonlinearities might be considered negligible in practice, they may introduce atypical behavior that would not be predicted by linear system analysis.

Nonlinear Structural Damping

Even linear aeroelastic models often use empirical models of structural damping; thus, little is known fundamentally about how to model structural damping for LCO. However an interesting and insightful hypothesis has been offered by Chen et al.[83] If one assumes that the structural damping increases with amplitude of structural motion (there is some experimental evidence to suggest this may be the case), and if the negative aerodynamic damping associated with flutter remains sufficiently small beyond the flutter boundary, then the nonlinear increase in structural damping may offset the negative aerodynamic damping, and this will lead to a nonlinear, neutrally stable motion, that is, LCO. Chen et al.[83] have performed calculations based upon this hypothesis that appear consistent with some of the LCO observed in the F-16 aircraft.

Large Shock Motions and Flow Separation

These aerodynamic nonlinearities are both the most difficult to model theoretically and also to investigate experimentally. Hence, it is perhaps not surprising that our correlations between theory and experiment are not yet what we might like them to be. As a corollary, observe that it will in all likelihood be easier to design a favorable nonlinear structural element to produce a benign LCO than to assure that flow nonlinearities will always be beneficial with respect to LCO.

NACA 64A010A conventional airfoil models.   In Fig. 16, recent results are shown for the LCO of a NACA 64A010 airfoil in plunge and pitch as predicted by an Euler flow model (Kholodar et al.[84]). In Fig. 16 the LCO amplitude is plotted vs the FSI for a range of Mach number. As can be seen, the LCO is relatively weak (the curves are nearly vertical) for most Mach numbers. For those Mach numbers where the LCO is relatively strong, it can be either benign
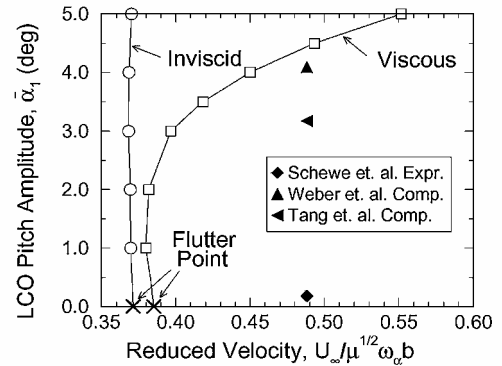

Fig. 17   LCO response amplitude vs (reduced) flow velocity: comparison of inviscid and viscous flow models for NLR 7301 supercritical airfoil.

(the curves bend to the right) or detrimental (the curves bend to the left) leading to LCO below the flutter boundary. This example also points out the substantial amount of data needed to assess LCO under these circumstances. A Navier–Stokes model has also been used to assess LCO of this configuration for a more limited range of parameters. The results (not shown) indicate a modest effect of viscosity provided that the mean angle of attack is sufficiently small and no flow separation occurs.

National Aerospace Laboratory (NLR) 7301 supercritical airfoil models.   Another configuration of interest is the supercritical airfoil, National Aerospace Laboratory (NLR) 7301, which has been studied experimentally by Knipfer and Schewe,[85] Schewe and Deyhle,[86] Schewe et al.[87,88] This has in turn inspired several theoretical studies using either an Euler or a Navier–Stokes flow model. A correlation among several theoretical models and the result of experiment is shown in Fig. 17. Figure 17 is from Thomas et al.,[89] who used a harmonic balance LCO solution method. Results are also shown from Weber et al.[90] and Tang et al.[91] where the more computationally demanding time-marching technique was used. Note that there is only a single data point from the latter, as is the case from the experiment. However, it is clear that to have a more meaningful correlation it is highly desirable to provide results for LCO amplitude over a range of FSI and Mach numbers. Hence, it is not yet clear what the conclusion should be with respect to correlation between theory and experiment. It does appear that the several theoretical results are in reasonable agreement. More correlations with the experimental data are needed.

Computational conditions are sensitive, and care must be taken to achieve reasonable steady initial pressure distributions for this configuration. Also, the LCO conditions appear to be very sensitive to details of the computations. Tang et al.[91] give results from the CFL3D-NS code illustrating effects of turbulence models, single-block and multi-block (parallel), multigrid subiterations, and time step. Agreement between theory and experiment for the LCO motion amplitudes has been difficult to achieve for this case, even including the effects of wind-tunnel wall interference (see Castro et al.[92]).

AGARD 445.6 wing models.   The AGARD 445.6 wing has been discussed earlier in terms of its flutter boundary; now we turn to very recent results from Thomas et al.[93] for LCO. The correlation between theory and experiment for the flutter boundary is again shown in Fig. 18, where the Euler flow model is that of Thomas et al. The flutter boundary correlation is consistent with that discussed earlier relative to Fig. 6. However, now we have in addition results for LCO amplitude vs FSI for various Mach number (Fig. 19). Note that a value of first mode nondimensional modal amplitude of $\xi = 0.012$ as shown in Fig. 19 corresponds to a wing tip deflection equal to one-fourth of the wing half-span. Note also that, in general, the LCO is predicted to be weak and there is no Mach number for which a benign LCO is predicted. Indeed, the strongest LCO is detrimental and occurs at the low supersonic Mach numbers, $M = 1.141$ and
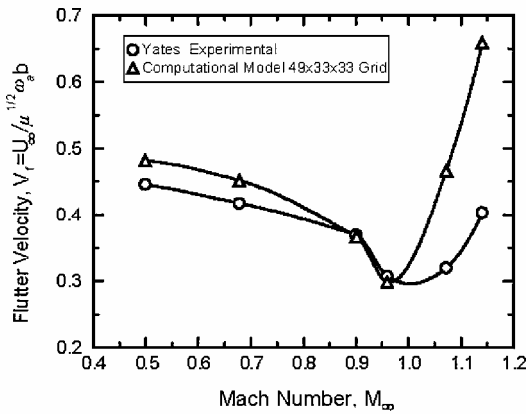
Fig. 18   FSI vs Mach number for AGARD wing 445.6: comparison of theory and experiment.
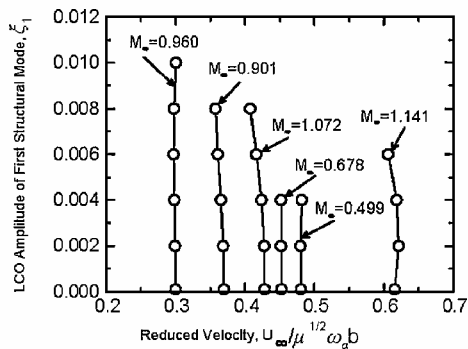

Fig. 19   LCO amplitude vs FSI (reduced velocity) for various Mach numbers for AGARD 445.6 wing.

1.072. This means that LCO may occur below the flutter boundary at these two Mach numbers, and perhaps this explains at least in part why flutter (or really an unstable LCO) occurred in the experiment below the predicted flutter boundary.

Small-amplitude LCO behavior for the AGARD 445.6 wing has also been calculated by Edwards.[94] The majority of published calculations for this wing model (actually a series of models with similar planforms) are for the weakened model #3 tested in air because this test covered the largest transonic Mach number range and showed a significant transonic dip in the flutter boundary. The focus on this particular configuration may be in some ways unfortunate, in that the model tested in air resulted in unrealistically large mass ratios and small reduced frequencies. Weakened models 5 and 6 were tested in heavy gas and had smaller mass ratios and higher reduced frequencies. Very good agreement was obtained with experiment for flutter speed index using the CAP-TSDV code over the Mach number range tested. For the highest Mach number tested, $M = 0.96$, it was noted that damping levels extracted from the computed transients were amplitude dependent, an indicator of nonlinear behavior. It was also found that small-amplitude divergent (in time) responses used to infer the flutter boundary would transition to LCO when the calculation was continued further in time. The wing-tip amplitude of the LCO was approximately 0.12 in. peak-to-peak, a level that is unlikely to be detected in wind-tunnel tests given the levels of model response to normal wind-tunnel turbulence.

Models for Aeroelastic Validation Involving Computation (MAVRIC) wing flutter model.   This business jet wing–fuselage model (Edwards[95,96]) was chosen by NASA Langley Research Center's Models for Aeroelastic Validation Involving Computation (MAVRIC) project with the goal of obtaining experimental wind-tunnel data suitable for CAE code validation at transonic separation onset conditions. LCO behavior was a primary target. An inexpensive construction method of stepped-thickness aluminum plate
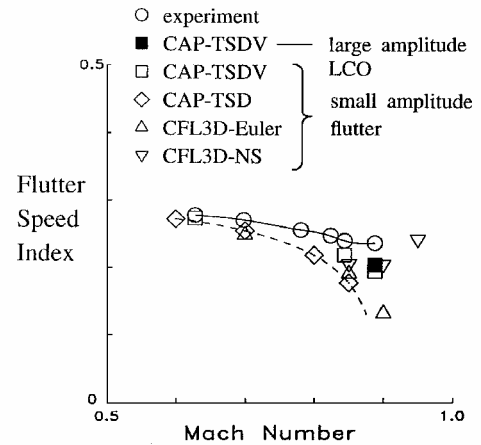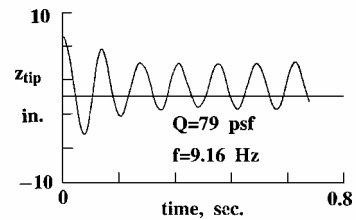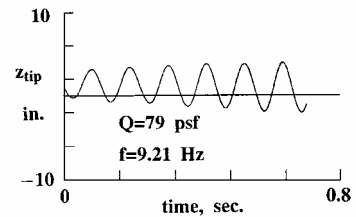

Fig. 20   FSI vs Mach number for MAVRIC model.

a) Amplitude decaying to LCO

b) Amplitude growing to LCO

Fig. 21   Transient response leading to a LCO: simulation for MAVRIC wing.

covered with end-grain balsa wood and contoured to the desired wing profile was used. A significant benefit of this method was the additional strength of the plate that enabled the model to withstand large amplitude LCO motions without damage.

The model was instrumented with three chords of unsteady pressure transducers and eight accelerometers. It was tested in air and in heavy gas and with three wing-tip configurations: clean, winglet, and pencil tipstore. Figure 20 shows the FSI boundary vs Mach number from an earlier test of this model (Edwards[?]), including computed CAE code comparisons. The experimental flutter boundary shows a gradual decrease in dynamic pressure, reaching a minimum at $M = 0.89$. The structural modifications and added instrumentation for the MAVRIC model had very little effect on the flutter boundary. Both the transonic small disturbance CAP-TSD(V) and the higher level CFL3D codes are in good agreement with experiment at the lower Mach numbers. Both inviscid codes, CAP-TSD and CFL3D-Euler, increasingly depart from experimental values, approaching the minimum FSI value. This emphasizes the necessity of the inclusion of viscous shock–boundary-layer interaction effects for LCO-like motions. Both viscous codes, CAP-TSDV and CFL3D-NS, are in good agreement with experiment at $M = 0.89$, where small-amplitude, time-marching responses were used to identify the flutter boundary.

The behavior of the MAVRIC model as flutter was approached during the wind-tunnel test indicated that wing motions tended to settle to a large-amplitude LCO condition, especially in the Mach number range near the minimum FSI conditions. Figure 21 demonstrates[96] the ability of the CAP-TSDV code to simulate these large-amplitude LCO motions. Large and small initial condition
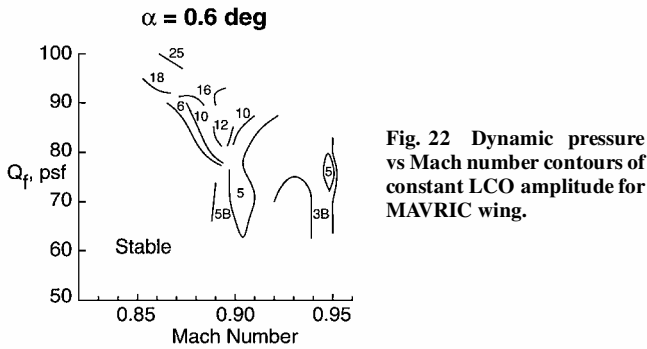
Fig. 22 Dynamic pressure vs Mach number contours of constant LCO amplitude for MAVRIC wing.

disturbance transient responses clearly show the 6-in. peak-to-peak wing-tip motions observed in the tests. Such large-amplitude aeroelastic motions have not been demonstrated by RANS codes, which have difficulty maintaining grid cell structure for significant grid deformations. Figure 22 shows the map of the regions of LCO found in the MAVRIC test in the vicinity of the minimum FSI (clean wing tip, $\alpha = 6$ deg) (Ref. 96). Numbers for the several contours in Fig. 22 give the half-amplitude of wing-tip LCO motions (gravitational acceleration) in the indicated regions. Two regions, B, are regions where beating vibrations were observed. For this test condition, wing motions are predominantly of the wing first bending mode at a frequency of 7–8 Hz. (Wind-off modal frequency is 4.07 Hz.) Two chimney features are seen, at $M \sim 0.91$ and at $M \sim 0.94$. Edwards[95] discusses flutter model responses that are indicative of more complex nonlinear behaviors than are commonly attributed to LCO. Thus, flutter-test engineers are familiar with responses such as bursting and beating, commonly used as indicators of the approach to flutter (and LCO).

Clipped-tip delta wing control surface buzz model. Parker et al.[97] describe a test of a clipped-tip delta wing model with a full span control surface. The leading-edge sweep was 60 deg, the biconvex wing profile had thickness of 3% of local chord, and the constant chord control surface length was approximately 13% of the root chord. The control surface was mounted on two flexure springs. The tests were conducted in air, which is of concern because there are known to be severe Reynolds number and/or transition effects for this tunnel at dynamic pressures below 50–75 psf (Ref. 95). Pak and Baker[98] have performed computational studies of this case. They compare the experimental buzz boundary with time-marching transient responses calculated with the CFL3D-NS code and the CAP-TSDV code, respectively. Both codes capture LCO behavior near the experimental buzz conditions with the higher level code appearing to have better agreement for the experimental trend vs Mach number. The responses offer excellent insight into issues and problems of the use of CAE time-marching codes for LCO-like studies. The record lengths of a number of the responses, which are extremely expensive to compute, are not sufficient for clear determination of the response final status. Also, LCO behaviors can result from very delicate force balances, and settling times to final LCO states can require many cycles of oscillation.

Residual pitch oscillations on the B-2. The B-2 bomber encountered a nonlinear aeroelastic residual pitch oscillation (RPO) during low-altitude, high-speed flight.[13] Neither the RPO nor any tendency of lightly damped response had been predicted by wholly linear aeroelastic design methods. The RPO involved symmetric wing bending modes and rigid-body degrees of freedom. It was possible to augment the CAP-TSDV aeroelastic analysis code with capability for the longitudinal short-period rigid-body motions, vehicle trim, and the full-time active flight control system including actuator dynamics. This computational capability enabled the analysis of the heavyweight, forward center of gravity flight condition.[13] The simulation predicts open-loop instability at $M = 0.775$ and closed-loop instability at $M = 0.81$, in agreement with flight test. To capture the limit-cycle behavior of the RPO, it was necessary to include

modeling of the nonlinear hysteretic response characteristic of the B-2 control surfaces for small-amplitude motions. This is caused by the small overlap of the servohydraulic control valve spool flanges with their mating hydraulic fluid orifices. With this realistic actuator modeling also included, limited amplitude RPO motions similar to those measured in flight were simulated. A lighter weight flight-test configuration exhibited very light damping near $M = 0.82$, but did not exhibit fully developed RPO. Instead, damping increased with slight further increase in speed, typical of hump mode behavior. The CAP-TSDV simulations did not capture this hump mode behavior.

Rectangular Goland wing model with tip store. Next in this section is a discussion of the recent and valuable papers by Beran et al.[99] and Huttsell et al.[100] In the paper by Beran et al.,[99] comparisons were made between the predictions of a fully nonlinear potential flow plus boundary-layer model (CAP-TSDV) and the results from classical fully linear theory (doublet lattice). The Goland wing which is a rectangular planform with a 4% parabolic arc airfoil, was used for this study. In Fig. 23, flutter boundaries and what is termed a LCO boundary are shown for the two theoretical methods. Results for the wing alone and for a wing with a tip store are given. Beran et al. note that for this configuration the aerodynamic effect of the tip store is small, but the effect of tip store dynamics (inertia) is important, as seen in Fig. 23. Note also that the two flow models give results in good agreement for the subsonic Mach number range, but differ substantially in the transonic range.

Beran et al.[99] distinguish between the flutter boundary (for the wing plus tip store) and the LCO boundary. However, based on the work of others, for example, Kholodar et al.[84] which shows that rapid changes in flutter (and LCO) modes may occur over small ranges of Mach number, it seems likely that these are both flutter boundaries per se. However, at the subsonic Mach number it is likely that no LCO was observed in these time simulations because the LCO is very weak. That is, at subsonic Mach numbers, the time simulation shows a rapidly exponentially diverging oscillation typical of a linear dynamic system. However, LCO was observed over a narrow range of transonic Mach numbers (again consistent with the findings of other investigators[84] for other configurations), where the aerodynamic nonlinearity is strong enough that a time simulation will reach a finite steady-state LCO amplitude in a reasonable amount of computational time. However, if the initial disturbance to the system is small enough or there is little hysteresis in the dependence of LCO steady-state amplitude on speed index, then the boundary for the onset of LCO should be essentially the same as the flutter boundary. There is some hysteretic LCO behavior for this configuration, as is discussed further in the paragraph after next.
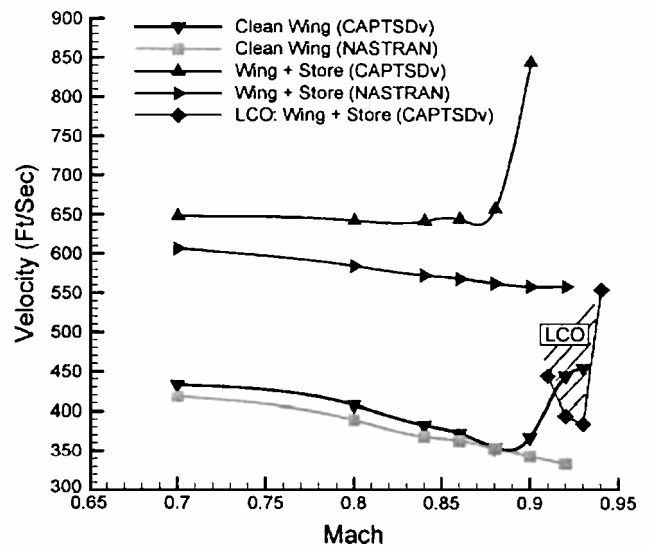

Fig. 23 Flutter and LCO boundaries: velocity vs Mach number for Goland wing.
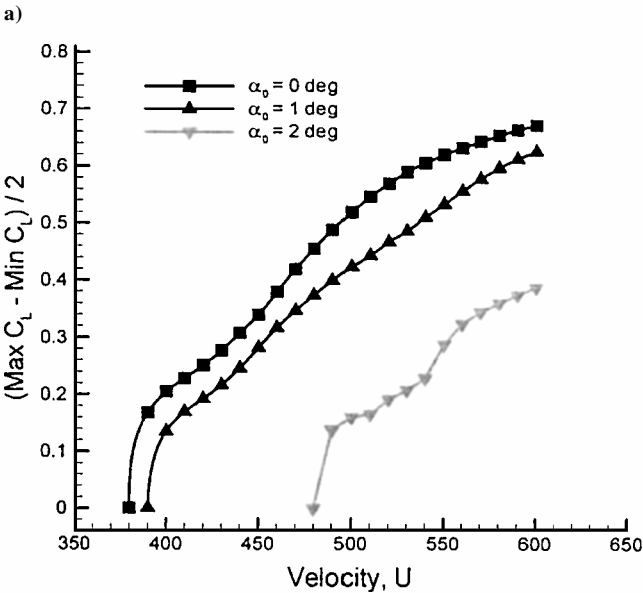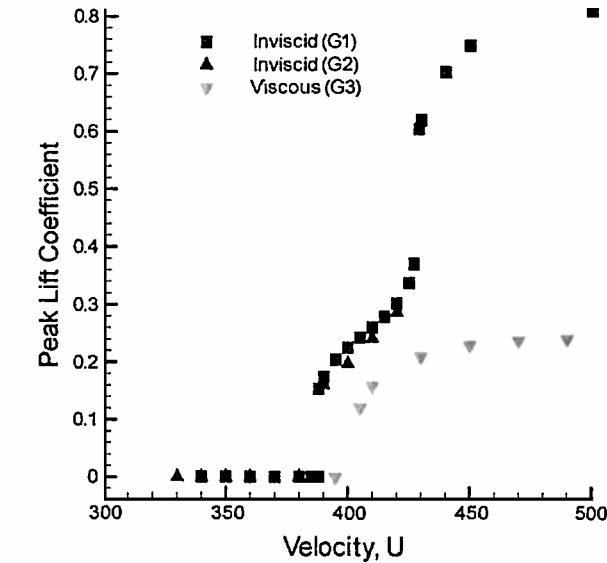
a)

b)

Fig. 24   LCO response vs flow velocity for Goland wing.

Fig. 25   LCO response vs flow velocity: an example of hysteresis for Goland wing.

In Fig. 24a, the LCO amplitude (in terms of oscillating aero-dynamic lift) is shown as a function of flow velocity for various theoretical models. Results are shown with and without store aero-dynamics (again the differences are small) and with and without the effects of viscosity. As can be seen, there is little effect of viscosity on the flow velocity at the onset of flutter and LCO, but the effect on LCO amplitude per se is substantial. (The abrupt increase in LCO response for the inviscid model may be indicative of unrealistic shock motions.) Recall the results of Thomas et al.[89] for the NLR 7301 airfoil, which showed similar behavior when comparing LCO response from inviscid and viscous flow models. Also recall the re-sults of Bohbot and Darracq[54] for the Isogai[48] case A, which show a similar effect.

In Fig. 24b, inviscid flow results are shown for various mean angles of attack. The results are qualitatively similar, but the effect of increased angle of attack is to increase the flow velocity at which flutter and LCO occur.

In Fig. 25, the results of Fig. 24a are shown again for increasing flow velocity [perturbed rigid initial condition (IC)] and decreasing flow velocity (path following IC). The results display hysteresis with the LCO amplitude observed being path dependent. As the flow velocity is increased and given a sufficiently small IC disturbance, no flutter or LCO is seen until a velocity of about 390 ft/s, but when the airfoil is then allowed to oscillate in the LCO and the
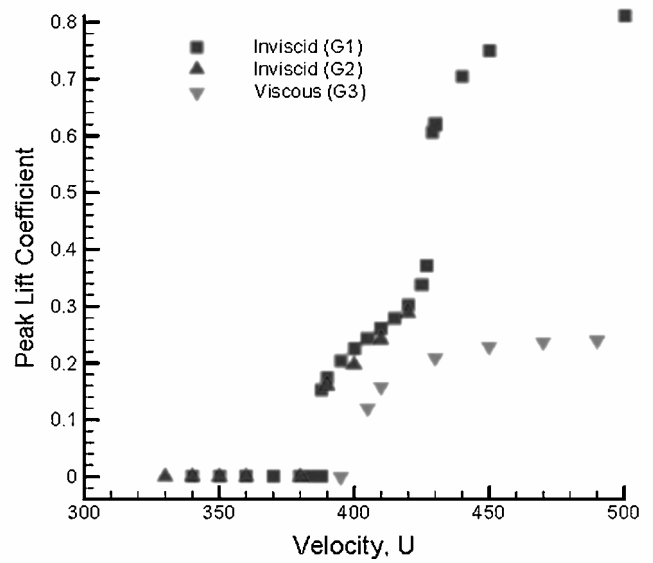
flow velocity is decreased, LCO continues until a lower velocity is reached of about 385 ft/s. Although the range of flow velocity over which hysteresis is observed is relatively small in this example, there is every reason to expect that for other parameter choices the range of hysteresis can be greater.

Time-marching codes compared to various experimental results.
In the paper by Huttsell et al.[100] several state-of-the-art time-marching CFD codes are used to investigate flutter and LCO for challenging cases drawn from flight or wind-tunnel tests. The CAP-TSD, CAP-TSDV, CFL3D, and ENS3DAE codes are all used. The results are extremely helpful in providing a realistic assessment of the state of the art of these codes, and they are also indicative future needs and improvements. For the F-15 aircraft example, difficulty was encountered in producing a computational grid with negative volumes being encountered. For the AV8-B aircraft, a steady-state flowfield could not be found due to oscillations in the numerical solver from one iteration to the next. These difficulties are not un-usual for CFD codes in the present authors' experience. Sometimes the difficulty in achieving a steady flow solution is attributed to shedding in the flowfield, but in the absence of a full nonlinear dynamic CFD calculation, that must remain a speculation. For the B-2 aircraft example, encouraging agreement was obtained for the frequency and damping variation of the critical flutter (and LCO) mode as a function of flight speed using the CAP-TSDV code. For the B-1, estimates of the damping associated with LCO were com-puted using the CFL3DAE code and favorably compared to those found in wind-tunnel tests. It is not entirely clear what the damping of an LCO means, however, because by definition LCO is a neu-trally stable motion. Two control surface buzz cases were consid-ered, and CFL3DAE had some success in predicting the behavior observed in the wind tunnel for a National Aerospace Plane-like configuration.

As Huttsell et al. note, additional work is needed to improve CFD model robustness, computational efficiency and grid deformation strategies.

Abrupt Wing Stall
Although not usually classified as a nonlinear aeroelastic response or LCO, abrupt wing stall (AWS) appears to share some of the same basic characteristics. A joint U.S. Navy/NASA/U.S. Air Force pro-gram over the last several years has addressed this class of phe-nomena (see Woodson[101]). Chambers[102] has presented a valuable historical account of AWS and drawn lessons learned from a num-ber of aircraft programs. Much of the recent work on AWS has been motivated by experiences with the F-18.

Briefly, AWS is encountered when the aircraft is at a sufficiently high angle of attack for flow separation to occur and the flow then begins to oscillate, including shock oscillations if the local Mach number is large enough. For large angles of attack, sonic conditions may be reached locally even for relatively low freestream Mach numbers. This oscillating flow may be asymmetric from one wing to the other, and therefore, the aircraft will roll. If this rolling motion is a transient, the motion is usually called wing drop, whereas if it is periodic in the roll angle, it is called wing rock. Wing rock has been modeled Nayfeh et al.[103] and Ericsson[104] as a LCO due to nonlinear self-excited coupling between the aerodynamic flow and the rolling motion of the aircraft. Wing drop has been modeled by including this effect by Kokolios and Cook,[105] who also include the oscillating aerodynamic rolling moment that may occur even in the absence of aircraft motion. This oscillating aerodynamic moment is due to a nonlinear self-excitation of the flow in the absence of aircraft motion, and thus, this moment is an external excitation as far as the vehicle motion is concerned. Because the dominant aircraft motion is rigid-body roll rather than the an elastic structural mode of the wing, for example, abrupt wing stall is not usually thought of as being an aeroelastic issue per se. Yet from a dynamics perspective, many of the issues with respect to aerodynamic modeling and aircraft motion are similar to those nonlinear phenomena discussed earlier in this paper. Valuable free-to-roll wind-tunnel model studies have been performed at NASA Langley Research Center (Lamar et al.[106]) as have some CFD simulations of AWS. Several sessions and papers devoted to this topic were presented at the recent 2003 AIAA Aerospace Sciences Meeting.

Uncertainty Due to Nonlinearity

There has been recent and renewed interest in the impact of uncertainties on aerospace system response. Here two scenarios that have been reported by operators of current aerospace systems are discussed, and the relationship of uncertainty to nonlinearity is noted.

Scenario 1

One scenario that has been reported is the following. An aircraft in straight and level flight does not experience flutter or LCO; however, when the aircraft is maneuvered LCO does occur, and then when the aircraft is returned to straight and level flight, the LCO persists. The question is, how has the maneuver generated LCO that persists in straight and level flight when LCO did not occur before the maneuver?

Within the framework of a linear aeroelastic model, such behavior is not possible, but an explanation is possible for a nonlinear aeroelastic system as a result of hysteresis. That is, if the disturbance to a nonlinear system is sufficiently small, LCO will not occur, but if a sufficiently large disturbance is applied to the system, for example, a maneuver, then LCO may be induced. Once LCO exists, it may persist due to hysteresis even if one returns to the nominal original flight condition. Such behavior has been observed in both mathematical and experimental wind-tunnel models where the nonlinear effect producing the LCO and hysteretic response is due to either structural freeplay or flow separation.

In this scenario, the uncertainty is because two different nonlinear response states are possible at the same parameter condition (flight speed and altitude) and the prior history of the system is critical in determining its response.

Scenario 2

In another scenario that has been observed, two distinct, but nominally identical systems (aircraft) are flown through the same trajectory, and one encounters LCO but the other does not. The question is, how is this possible? Again insights obtained from nonlinear aeroelastic models may offer an explanation.

Consider an aircraft with freeplay as an example. Now it is very difficult to maintain the same amount of freeplay in each and every aircraft. Then what might happen if two otherwise identical aircraft have different amounts of freeplay? For the aircraft with the smaller freeplay, the LCO amplitude (which scales in proportion to the magnitude of freeplay) might not be noticeable because it

is too small. However, for the aircraft with the larger freeplay, the LCO may be detectable. From recent theoretical and experimental studies of freeplay,[60] not only is it known that LCO amplitudes increase in proportion to the magnitude of the freeplay, but also that the magnitude of the angle of attack required to suppress LCO due to freeplay scales in proportion to the magnitude of the freeplay. Thus, the aircraft with the larger freeplay will not only have a LCO of larger amplitude, but it will also experience freeplay over a larger range of angle of attack, again making it more likely that LCO will be observed.

These two scenarios and their possible explanation point up the importance of developing a fundamental understanding of the underlying structural and fluid nonlinearities that may occur in aeroelastic systems in dealing with the uncertainties and apparent paradoxes that have been observed in practice.

Conclusions

Substantial progress has been made in modeling and understanding nonlinear aeroelastic phenomena. Experimental and theoretical investigations have shown good correlation for a number of nonlinear physical mechanisms. As a broad generalization, one may say that our understanding of and correlation among alternative theoretical models and experiment is further advanced for nonlinear structural mechanisms, such as freeplay and large deflection geometric nonlinearities of beams and plates, than it is for nonlinear fluid mechanisms, such as large shock motions and separated flows. Nevertheless, accurate and much more computationally efficient theoretical models are now becoming available for nonlinear aerodynamic flows, and there is cause for optimism in addressing these issues going forward.

As has been emphasized throughout this paper, a number of physical mechanisms can lead to nonlinear aeroelastic response including the impact of static (steady flow) fluid or static structural nonlinearities in changing the flutter boundary of an aeroelastic system. Of course, dynamic nonlinearities play a critical role in the development of LCOs, hysteresis in flutter and LCO response, and the sensitivity of both to initial and external disturbances.

The good news for the flight vehicle designer is that, because of nonlinear aeroelastic effects, finite amplitude oscillations can in some cases replace what would otherwise be the rapidly growing and destructive oscillations of classical flutter behavior. A careful consideration and design of favorable nonlinearities offers a new opportunity for improved performance and safety of valuable wind-tunnel models, flight vehicles, and their operators and passengers. Once nonlinear aeroelastic models have reached a state of maturity sufficient for their consideration in the design process, then active and adaptive control can potentially provide for even greater flight vehicle performance. The discussion of active and adaptive control is beyond the scope of this paper, but the reader may wish to consult the recent literature on this topic.[107–115]

References

[1]Thompson, J. M. T., and Stewart, H. B., *Nonlinear Dynamics and Chaos*, Wiley, New York, 1988.

[2]Denegri, C. M., Jr., "Correlation of Classical Flutter Analyses and Nonlinear Flutter Responses Characteristics," International Forum on Aeroelasticity and Structural Dynamics, 1997, pp. 141–148.

[3]Denegri, C. M., Jr., and Cutchins, M. A., "Evaluation of Classical Flutter Analysis for the Prediction of Limit Cycle Oscillations," AIAA Paper 97-1021, April 1997.

[4]Denegri, C. M., Jr., "Limit-Cycle Oscillation Flight Test Results of a Fighter with External Stores," *Journal of Aircraft*, Vol. 37, No. 5, 2000, pp. 761–769.

[5]Denegri, C. M., Jr., and Johnson, M. R., "Limit-Cycle Oscillation Prediction Using Artificial Neural Networks," *Journal of Guidance, Control, and Dynamics*, Vol. 24, No. 5, 2001, pp. 887–895.

[6]AGARD Specialists Meeting on Wings-with-Stores Flutter, 39th Meeting of the Structures and Materials Panel, CP 162, AGARD, Oct. 1974.

[7]Bunton, R. W., and Denegri, C. M. Jr., "Limit-Cycle Oscillation Characteristics of Fighter Aircraft," *Journal of Aircraft*, Vol. 37, No. 5, 2000, pp. 916–918.

[8]Cunningham, A. M., Jr., "A Generic Nonlinear Aeroelastic Method with Semi-Empirical Nonlinear Unsteady Aerodynamics," Vols. 1 and 2, U.S. Air Force Research Lab., Rept. AFRL-VA-WP-R-1999-3014, Wright–Patterson AFB, OH, 1999.

[9]Cunningham, A. M., Jr., "The Role of Nonlinear Aerodynamics in Fluid-Structure Interactions," AIAA Paper 98-2423, 1998.

[10]Cunningham, A. M., Jr., and Geurts, E. G. M., "Analysis of Limit Cycle Oscillation/Transonic High Alpha Flow Visualization," U.S. Air Force Research Lab., Rept. AFRL-VA-WP-TR-1998-3003, Pt. 1, Wright–Patterson AFB, OH, Jan. 1998.

[11]Dobbs, S. K., Miller, G. D., and Stevenson, J. R., "Self Induced Oscillation Wind Tunnel Test of a Variable Sweep Wing," *26th AIAA/ASME/ASCE/AHS Structures, Structural Dynamics, and Materials Conference*, AIAA, Washington, DC, 1985.

[12]Hartwich, P. M., Dobbs, S. K., Arslan, A. E., and Kim, S. C., "Navier–Stokes Computations of Limit Cycle Oscillations for a B-1-Like Configuration," AIAA Paper 2000-2338, June 2000.

[13]Dreim, D. R., Jacobson, S. B., and Britt, R. T., "Simulation of Non-Linear Transonic Aeroelastic Behavior on the B-2," NASA CP-1999-209136, *CEAS/AIAA/ICASE/NASA Langley International Forum on Aeroelasticity and Structural Dynamics*, 1999, pp. 511–521.

[14]Croft, J., "Airbus Elevator Flutter: Annoying or Dangerous?," *Aviation Week and Space Technology*, Aug. 2001.

[15]Dowell, E. H., *Aeroelasticity of Plates and Shell*, Kluwer Academic, Norwell, MA, 1975.

[16]Dowell, E. H., *Panel Flutter*, NASA SP-8004, 1972.

[17]Yurkovich, R. N., Liu, D. D., and Chen, P. C., "The State-of-the-Art of Unsteady Aerodynamics for High Performance Aircraft," AIAA Paper 2001-0428, Jan. 2001.

[18]Dowell, E. H., and Hall, K. C., "Modeling of Fluid–Structure Interaction," *Annual Review of Fluid Mechanics*, Vol. 33, 2001, pp. 445–490.

[19]Bennett, R. M., and Edwards, J. W., "An Overview of Recent Developments in Computational Aeroelasticity," AIAA Paper 98-2421, June 1998.

[20]Beran, P., and Silva, W., "Reduced-Order Modeling: New Approaches for Computational Physics," AIAA Paper 2001-0853, Jan. 2001.

[21]Kim, T., and Bussoletti, J. E., "An Optimal Reduced Order Aeroelastic Modeling Based on a Response-Based Modal Analysis of Unsteady CFD Models," AIAA Paper 2001-1525, April 2001.

[22]Silva, W. A., "Application of Nonlinear Systems Theory to Transonic Unsteady Aerodynamic Responses," *Journal of Aircraft*, Vol. 30, No. 5, 1993, pp. 660–668.

[23]Silva, W. A., "Extension of a Nonlinear System Theory to General-Frequency Unsteady Transonic Aerodynamic Responses," *34th AIAA Structures, Structural Dynamics, and Materials Conference*, AIAA, Reston, VA, 1993, pp. 2490–2503.

[24]Silva, W. A., "Extension of a Nonlinear Systems Theory to Transonic Unsteady Aerodynamic Responses," AIAA Paper 93-1590, April 1993.

[25]Silva, W. A., "Discrete-Time Linear and Nonlinear Aerodynamic Impulse Responses for Efficient (CFD) Analyses," Ph.D. Dissertation, College of William and Mary, Williamsburg, VA, Oct. 1997.

[26]Silva, W. A., "Identification of Linear and Nonlinear Aerodynamic Impulse Response Using Digital Filter Techniques," *AIAA Atmospheric Flight Mechanics Conference*, AIAA, Reston, VA, 1997, pp. 584–597.

[27]Silva, W. A., "Reduced-Order Models Based on Linear and Nonlinear Aerodynamic Impulse Response," *International Forum on Aeroelasticity and Structural Dynamics*, NASA Langley Research Center, Hampton, VA, June 1999, pp. 369–379.

[28]Raveh, D., Levy, Y. and Karpel, M., "Aircraft Aeroelastic Analysis and Design Using CFD-Based Unsteady Loads," AIAA Paper 2000-1325, April 2000.

[29]Raveh, D. E., "Reduced-Order Models for Nonlinear Unsteady Aerodynamics," *AIAA Journal*, Vol. 39, No. 8, 2001, pp. 1417–1429.

[30]Farhat, C., Geuzaine, P., Brown, G., and Harris, C., "Nonlinear Flutter Analysis of an F-16 in Stabilized, Accelerated, and Increased Angle of Attack Flight Conditions," AIAA Paper 2002-1490, April 2002.

[31]Farhat, C., Harris, C., and Rixen, D., "Expanding a Flutter Envelope Using Accelerated Flight Data: Application to An F-16 Fighter Configuration," AIAA Paper 2000-1702, April 2000.

[32]Roughen, K. M., Baker, M. L., and Fogarty, T., "Computational Fluid Dynamics and Doublet-Lattice Calculation of Unsteady Control Surface Aerodynamics," *Journal of Guidance, Control and Dynamics*, Vol. 24, No. 1, 2001, pp. 160–166.

[33]Schuster, D. M., Edwards, J. W., and Bennett, R. M., "An Overview of Unsteady Pressure Measurements in the Transonic Dynamics Tunnel," AIAA Paper 2000-1770, April 2000.

[34]Ashley, H., "Role of Shocks in the 'Sub-Transonic' Flutter Phenomenon," *Journal of Aircraft*, Vol. 17, March 1980, pp. 187–197.

[35]Davis, S. S., and Malcolm, G. N., "Transonic Shock-Wave/Boundary-Layer Interactions on an Oscillating Airfoil," *AIAA Journal*, Vol. 18, No. 11, 1980, pp. 1306–1312.

[36]McMullen, M., Jameson, A., and Alonso, J. J., "Application of a Nonlinear Frequency Domain Solver to Euler and Navier–Stokes Equations," AIAA Paper 2002-0120, Jan. 2002.

[37]Kreiselmaier, E., and Laschka, B., "Small Disturbance Euler Equations: Efficient and Accurate Tool for Unsteady Load Prediction," *Journal of Aircraft*, Vol. 37, No. 5, 2000.

[38]Ruiz-Calavera, L. P. (ed.), *Verification and Validation Data for Computational Unsteady Aerodynamics Codes*, Research and Technology Organization, Rept. TW-26, 2000.

[39]Farhat, C., and Lesoinne, M., "Enhanced Partitioned Procedures for Solving Nonlinear Transient Aeroelastic Problems," AIAA Paper 98-1806, April 1998.

[40]Raveh, D. E., Levy, Y., and Karpel, M., "Efficient Aeroelastic Analysis Using Computational Unsteady Aerodynamics," *Journal of Aircraft*, Vol. 38, No. 3, 2001, pp. 547–556.

[41]Thomas, J. P., Dowell, E. H., and Hall, K. C., "Three-Dimensional Transonic Aeroelasticity Using Proper Orthogonal Decomposition Based Reduced Order Models," AIAA Paper 2001-1526, April 2001.

[42]Gupta, K. K., "Development of a Finite Element Aeroelastic Analysis Capability," *Journal of Aircraft*, Vol. 33, No. 5, 1996, pp. 995–1002.

[43]Scott, R. C., Silva, W. A., Florance, J. R., and Keller, D. F., "Measurement of Unsteady Pressure Data on a Large HSCT Semi-Span Wing and Comparison with Analysis," AIAA Paper 2002-1648, 2002.

[44]Silva, W. A., Keller, D. F., Florance, J. R., Cole, S. R., and Scott, R. C., "Experimental Steady and Unsteady Aerodynamic and Flutter Results for HSCT Semi-span Models," AIAA Paper 2000-1697, April 2000.

[45]Bennett, R. M., Eckstrom, C. V., Rivera, J. A., Jr., Danberry, B. E., Farmer, M. G., and Durham, M. H., "The Benchmark Aeroelastic Models Program: Description and Highlights of Initial Results," NASA TM 104180, April 1991.

[46]Bennett, R. M., Scott, R. C., and Wieseman, C. D., "Computational Test Cases for the Benchmark Active Controls Model," *Journal of Guidance, Control, and Dynamics*, Vol. 23, No. 5, 2000, pp. 922–929.

[47]Bartels, R. E., and Schuster, D. M., "A Comparison of Two Navier–Stokes Aeroelastic Methods Using BACT Benchmark Experimental Data," *Journal of Guidance, Control, and Dynamics*, Vol. 23, No. 5, 2000, pp. 1094–1099.

[48]Isogai, K., "On the Transonic-Dip Mechanism of Flutter of Sweptback Wing," *AIAA Journal*, Vol. 17, No. 7, 1979, pp. 793–795.

[49]Hall, K. C., Thomas, J. P., and Dowell, E. H., "Reduced-Order Modeling of Unsteady Small Disturbance Flows Using a Frequency-Domain Proper Orthogonal Decomposition Technique," AIAA Paper 99-0655, Jan. 1999.

[50]Hall, K. C., Thomas, J. P., and Dowell, E. H., "Proper Orthogonal Decomposition Technique for Transonic Unsteady Aerodynamic Flows," *AIAA Journal*, Vol. 38, No. 10, 2000, pp. 1853–1862; also AIAA Paper 99-0655, Oct. 2000.

[51]Ehlers, F. E., and Weatherhill, W. H., "A Harmonic Analysis Method for Unsteady Transonic Flow and Its Application to the Flutter of Airfoils," NASA CR-3537, May 1982.

[52]Edwards, J. W., Bennett, R. M., Whitlow, W., Jr., and Seidel, D. A., "Time-Marching Transonic Flutter Solutions Including Angle-of-Attack Effects," *Journal of Aircraft*, Vol. 20, No. 11, 1983, pp. 899–906.

[53]Prananta, B. B., Hounjet, J. H. L., and Zwaan, R. J., "Two-Dimensional Transonic Aeroelastic Analysis Using Thin-Layer Navier–Stokes Methods," *Journal of Fluids and Structures*, No. 12, 1998, pp. 655–676.

[54]Bohbot, J., and Darracq, D., "Time Domain Analysis of Two D.O.F. Airfoil Flutter Using an Euler/Turbulent Navier–Stokes Implicit Solver," *International Forum on Structural Dynamics*, Vol. 2, 2001, pp. 75–86.

[55]Bendiksen, O. O., "Energy Approach to Flutter Suppression and Aeroelastic Control," *Journal of Guidance, Control and Dynamics*, Vol. 24, No. 1, 2001, pp. 176–184.

[56]Bendiksen, O. O., "Transonic Flutter," AIAA Paper 2002-1488, April 2002.

[57]Bendiksen, O. O., "Transonic Flutter and the Nature of the Transonic Dip," *International Forum on Structural Dynamics 2001*, Vol. 11, 2001.

[58]Dogget, R. V., Jr., Rainey, A. G., and Morgan, H. G., "An Experimental Investigation of Aerodynamic Effects of Airfoil Thickness on Transonic Flutter Characteristics," NASA TM X-79, 1959.

[59]Dowell, E. H., Crawley, E. F., Curtiss, H. C., Jr., Peters, D. A., Scanlan, R. H., and Sisto, F., *A Modern Course in Aeroelasticity*, 3rd ed. Kluwer Academic, Dordrecht, The Netherlands, 1995, p. 699.

[60]Dowell, E. H., and Tang, D., "Nonlinear Aeroelasticity and Unsteady Aerodynamics," AIAA Paper 2002-0003, Jan. 2002.

[61]O'Neil, T., Gilliat, H., and Strganac, T., "Investigation of Aeroelastic Response for a System with Continuous Structural Nonlinearities," AIAA Paper 96-1390, 1996.

[62]Block, J. J., and Strganac, T. W., "Applied Active Control for a Nonlinear Aeroelastic Structure," *Journal of Guidance, Control, and Dynamics*, Vol. 21, No. 6, 1998, pp. 838–845.

[63]Ko, J., Kurdila, A. J., and Strganac, T. W., "Nonlinear Control of a Prototypical Wing Section with Torsional Nonlinearity," *Journal of Guidance, Control, and Dynamics*, Vol. 20, No. 6, 1997, pp. 1181–1189.

[64]Ko, J., Strganac, T. W., and Kurdila, A. J., "Adaptive Feedback Linearization for the Control of a Typical Wing Section with Structural Nonlinearity," *Nonlinear Dynamics*, Vol. 18, No. 3, 1999, pp. 289–301.

[65]Ko, J., Strganac, T. W., and Kurdila, A. J., "Stability and Control of a Structurally Nonlinear Aeroelastic System," *Journal of Guidance, Control, and Dynamics*, Vol. 21, No. 5, 1998, pp. 718–725.

[66]Thompson, D. E., and Strganac, T. W., "Store-Induced Limit Cycle Oscillations and Internal Resonance in Aeroelastic Systems," AIAA Paper 2000-1413, 2000.

[67]Cole, S. R., "Effects of Spoiler Surfaces on the Aeroelastic Behavior of a Low-Aspect Ratio Wing," *31st AIAA Structures, Structural Dynamics, and Materials Conference*, AIAA, Washington, DC, 1990, pp. 1455–1463.

[68]Oh, K., Nayfeh, A. H., and Mook, D. T., "Modal Interactions in the Forced Vibration of a Cantilever Metallic Plate," *Nonlinear and Stochastic Dynamics*, Vol. 192, 1994, pp. 237–247.

[69]Pai, P. F., and Nayfeh, A. H., "Three-Dimensional Nonlinear Vibrations of Composite Beams—I: Equations of Motion," *Nonlinear Dynamics*, Vol. 1, 1990, pp. 477–502.

[70]Stearman, R. O., Powers, E. J., Schwarts, J., and Yurkorvich, R., "Aeroelastic System Identification of Advanced Technology Aircraft Through Higher Order Signal Processing," *9th International Modal Analysis Conference*, 1991, pp. 1607–1616.

[71]Gilliatt, H. C., Strganac, T. W., and Kurdila, A. J., "Nonlinear Aeroelastic Response of an Airfoil," *35th Aerospace Sciences Meeting and Exhibit*, AIAA, Reston, VA, 1997, pp. 258–266.

[72]Chang, J. H., Stearman, R. O., Choi, D., and Powers, E. J., "Identification of Aeroelastic Phenomenon Employing Bispectral Analysis Techniques," *International Modal Analysis Conference and Exhibit*, Vol. 2, 1985, pp. 956–964.

[73]Gordnier, R. E., and Melville, R. B., "Physical Mechanisms for Limit-Cycle Oscillations of a Cropped Delta Wing," AIAA Paper 99-3796, June 1999.

[74]Gordnier, R. E., and Melville, R. B., "Numerical Simulation of Limit-Cycle Oscillations of a Cropped Delta Wing Using the Full Navier–Stokes Equations," *International Journal of Computational Fluid Dynamics*, Vol. 14, No. 3, 2001, pp. 211–224.

[75]Schairer, E. T., and Hand, L. A., "Measurement of Unsteady Aeroelastic Model Deformation by Stereo Photogrammetry," AIAA Paper 97-2217, June 1997.

[76]Preidikman, S., and Mook, D. T., "Time Domain Simulations of Linear and Nonlinear Aeroelastic Behavior," *Journal of Vibration and Control*, Vol. 6, No. 8, 2000, pp. 1135–1175.

[77]Patil, M. J., Hodges, D. H., and Cesnik, C., "Nonlinear Aeroelasticity and Flight Dynamics of High-Altitude Long-Endurance Aircraft," AIAA Paper 99-1470, 1999.

[78]Patil, M. J., Hodges, D. H., and Cesnik, C. E., "Nonlinear Aeroelastic Analysis of Complete Aircraft in Subsonic Flow," *Journal of Aircraft*, Vol. 37, No. 5, 2000, pp. 753–760.

[79]Tang, D. M., and Dowell, E. H., "Effects of Angle of Attack on Nonlinear Flutter of a Delta Wing," *AIAA Journal*, Vol. 39, No. 1, 2001, pp. 15–21.

[80]Tang, D. M., and Dowell, E. H., "Experimental and Theoretical Study on Aeroelastic Response of High-Aspect-Ratio Wings," *AIAA Journal*, Vol. 39, No. 8, 2001, pp. 1430–1441.

[81]Kim, K., and Strganac, T., "Aeroelastic Studies of a Cantilever Wing with Structural and Aerodynamic Nonlinearities," AIAA Paper 2002-1412, April 2002.

[82]Crespo da Silva, M. R. M., and Glynn, C. C., "Nonlinear Flexural-Torsional Dynamics of Inextensional Beams-I: Equations of Motions," *Journal of Structural Mechanics*, ASCE, Vol. 6, No. 4, 1978, pp. 437–448.

[83]Chen, P. C., Sarhaddi, D., and Liu, D. D., "Limit Cycle Oscillation Studies of a Fighter with External Stores," AIAA Paper 98-1727, 1998.

[84]Kholodar, D. B., Thomas, J. P., Dowell, E. H., and Hall, K. C., "A Parametric Study of Transonic Airfoil Flutter and Limit Cycle Oscillation Behavior," *Journal of Aircraft* (to be published); also AIAA Paper 2002-1211, April 2002.

[85]Knipfer, A., and Schewe, G., "Investigations of and Oscillation Supercritical 2-D Wing Section in a Transonic Flow," AIAA Paper 99-0653, Jan. 1999.

[86]Schewe, G., and Deyhle, H., "Experiments on Transonic Flutter of a Two-Dimensional Supercritical Wing with Emphasis on the Nonlinear Effects," *Proceeding of the Royal Aeronautical Society Conference on Unsteady Aerodynamics*, London, U.K., 1996.

[87]Schewe, G., Knipfer, A., and Henke, H., "Experimentelle und numerisch Untersuchung zum transonischen Flügelflattern im Hinblick auf nichtlineare Effecte," unpublished manuscript, Feb. 1999.

[88]Schewe, G., Knipfer, A., Mai, H., and Dietz, G., "Experimental and Numerical Investigation of Nonlinear Effects in Transonic Flutter," English Version DLR German Aerospace Center, Final Rept. DLR IB 232-2002 J 01, translated by W. F. King III, corresponds to Final Rept. for BMBF, Nichtlineare Effekte beim transsonischen Flattern (FKZ 13 N 7172) and Internal Rept. DLR IB 2001 J03, Jan. 25, 2002.

[89]Thomas, J. P., Dowell, E. H., and Hall, K. C., "Modeling Viscous Transonic Limit Cycle Oscillation Behavior Using a Harmonic Balance Approach," AIAA Paper 2002-1414, April 2002.

[90]Weber, S., Jones, K. D., Ekaterinaris, J. A., and Platzer, M. F., "Transonic Flutter Computations for a 2-D Supercritical Wing," AIAA Paper 99-0798, Jan. 1999.

[91]Tang, L., Bartels, R. E., Chen, P. C., and Liu, D. D., "Simulation of Transonic Limit Cycle Oscillations Using a CFD Time-Marching Method," AIAA Paper 2001-1290, April 2001.

[92]Castro, B. M., Ekaterinaris, J. A., and Platzer, M. F., "Navier–Stokes Analysis of Wind-Tunnel Interference on Transonic Airfoil Flutter," *AIAA Journal*, Vol. 40, No. 7, 2002, pp. 1269–1276.

[93]Thomas, J. P., Dowell, E. H., and Hall, K. C., "A Harmonic Balance Approach for Modeling Three-Dimensional Nonlinear Unsteady Aerodynamics and Aeroelasticity," Paper IMECE-2002-32532, American Society of Mechanical Engineers, International Mechanical Engineering Conf. and Exposition, Nov. 2002.

[94]Edwards, J. W., "Calculated Viscous and Scale Effects on Transonic Aeroelasticity," *Numerical Unsteady Aerodynamic and Aeroelastic Simulation*, AGARD Rept. 822, March 1998.

[95]Edwards, J. W., Schuster, D. M., Spain, C. V., Keller, D. F., and Moses, R. W., "MAVRIC Flutter Model Transonic Limit Cycle Oscillation Test," AIAA Paper 2001-1291, April 2001.

[96]Edwards, J. W., "Transonic Shock Oscillations and Wing Flutter Calculated with an Interactive Boundary Layer Coupling Method," NASA TM-110284, Aug. 1996.

[97]Parker, E. C., Spain, C. V., and Soistmann, D. L., "Aileron Buzz Investigated on Several Generic NASP Wing Configurations," AIAA Paper 91-0936, April 1991.

[98]Pak, C., and Baker, M. L., "Control Surface Buzz Analysis of a Generic Nasp Wing," AIAA Paper 2001-1581, 2001.

[99]Beran, P. S., Khot, N. S., Eastep, F. E., Snyder, R. D., Zweber, J. V., Huttsell, L. J., and Scott, J. N., "The Dependence of Store-Induced Limit-Cycle Oscillation Predictions on Modeling Fidelity," RTO Applied Vehicle Technology Panel Symposium on Reduction of Military Vehicle Acquisition Time and Cost Through Advanced Modeling and Virtual Product Simulation, Paper 44, April 2002.

[100]Huttsell, L., Schuster, D., Volk, J., Giesing, J., and Love, M., "Evaluation of Computational Aeroelasticity Codes for Loads and Flutter," AIAA Paper 2001-569, 2001.

[101]Woodson, S. H., "Wing Drop," *McGraw–Hill 2002 Yearbook of Science and Technology*, McGraw–Hill, New York, 2001.

[102]Chambers, J. R., "Historical Review: Perspective on Experiences with Uncommanded Lateral Motions at High-Subsonic and Transonic Speeds," Ball Aerospace and Technologies Rept., Aerospace Systems Div., Feb. 1999.

[103]Nayfeh, A. H., Elzebda, J. M., and Mook, D. T., "Analytical Study of the Subsonic Wing-Rock Phenomenon for Slender Delta Wings," *Journal of Aircraft*, Vol. 26, No. 9, 1989, pp. 805–809.

[104]Ericsson, L. E., "Flow Physics Generating Highly Nonlinear Lateral Stability Characteristics of 65-Degree Delta–Wing–Body," *Journal of Aircraft*, Vol. 38, No. 5, 2001, pp. 932–934.

[105]Kokolios, A., and Cook, S. P., "Modeling Abrupt Wing Stall From Flight Test Data," 32nd Annual Symposium of the Society of Flight Test Engineers, Sept. 2001.

[106]Lamar, J. E., Hall, R. M., Sanders, E. N., Cook, S. P., and Grove, D. V., "Status and Plans of Abrupt Wing Stall Figures-of-Merit (FOM) Studies From Experimental and Computational Fluid Dynamics," NASA TR 2003, (in preparation).

[107]Heeg, J., "Analytical and Experimental Investigation of Flutter Suppression by Piezoelectric Actuation," NASA TP 3241, 1993.

[108]Lazarus, K. B., Crawley, E. F., and Lin, C. Y., "Fundamental Mechanism of Aeroelastic Control with Control Surface and Strain Actuation," *32nd AIAA/ASME/ASCE/AHS Structures, Structural Dynamics, and Materials Conference*, AIAA, Washington, DC, 1991, pp. 1817–1831.

[109]Lazarus, K. B., Crawley, E. F., and Lin, C. Y., "Multivariable Active Lifting Surface Control Using Strain Actuation: Analytical and Experimental Results," *Journal of Aircraft*, Vol. 34, No. 3, 1997, pp. 313–321.

[110]Vipperman, J. S., Barker, J. M., Clark, R. L., and Balas, G. S., "Comparison of μ- and H_2-Synthesis Controllers on an Experimental Typical Section," *Journal of Guidance, Control, and Dynamics*, Vol. 22, No. 2, 1999, pp. 278–285.

[111]Clark, R. L., Frampton, K. D., and Dowell, E. H., "Control of a Three-Degree-of-Freedom Airfoil with Limit-Cycle Behavior," *Journal of Aircraft*, Vol. 37, No. 3, 2000, pp. 533–536.

[112]Frampton, K. D., and Clark, R. L., "Experiments on Control of Limit-Cycle Oscillations in a Typical Section," *Journal of Guidance, Control, and Dynamics*, Vol. 23, No. 5, 2000, pp. 956–960.

[113]Rule, J. A., Richard, R. E., and Clark, R. L., "Design of an Aeroelastic Delta Wing Model for Active Flutter Control," *Journal of Guidance, Control, and Dynamics*, Vol. 24, No. 5, 2001, pp. 918–924.

[114]Richard, R. W., Rule, J. A., and Clark, R. L., "Genetic Spatial Optimization of Active Elements on an Aeroelastic Delta Wing," *Journal of Vibration and Acoustics*, Vol. 123, 2001, pp. 466–471.

[115]Platanitis, G., and Strganac, T., "Control of a Wing Section with Nonlinearities Using Leading and Trailing Edge Control Surfaces," AIAA Paper 2002-1718, April 2002.